Post-print of: (Paper) Dalton Trans. , 2012, 41, 14524-14539

DOI: 10.1039/C2DT31334K

Migratory insertion reactions of nickel and palladium σ-alkyl complexes with a phosphinito-imine ligand†‡

Laura Ortiz de la Tabla , Inmaculada Matas , Eleuterio Álvarez , Pilar Palma and Juan Cámpora

Instituto de Investigaciones Químicas. Consejo Superior de Investigaciones Científicas – Universidad de Sevilla, Américo Vespucio, 49, 41092, Sevilla, Spain. E-mail: ppalma@iiq.csic.es; campora@iiq.csic.es

Received 21st June 2012 , Accepted 3rd August 2012

First published on the web 6th August 2012

Ligand exchange reactions have been used for the synthesis of metallacyclic complexes of Ni and Pd of the type [M(CH2CMe2-*o*-C6H4)(P–N)], where P–N is the phosphinito-imine ligand P(iPr)2OC(Me)N(2,6-C6H3(iPr)2. The protic acid [H(OEt2)(BAr'4)] (Ar' = 3,5-C6H3(CF3)2) selectively cleaves one of the two σ metal–carbon bonds, affording cationic monoalkyl complexes. Nickel monoalkyls stabilized with Et2O or MeCN ligands are thermally unstable and spontaneously undergo a decomposition process that ultimately leads to the breakdown of the phosphinito-imine ligand. In contrast, cationic alkylpalladium derivatives are thermally very stable, allowing the isolation of a formally unsaturated monoalkyl complex stabilized by an intramolecular π-arene interaction. Although monoalkynickel and -palladium phosphinito-imine derivatives are inactive as ethylene polymerization or copolymerization catalysts, they readily experience migratory insertion reactions. A palladium chelate arising from the successive insertion of CO and ethylene has been isolated and characterized.

Introduction

The last two decades have witnessed a sustained interest in late transition metal catalysts for olefin oligomerization, polymerization and copolymerization.1–8 In the quest for finding successful ligand/metal combinations, a large number of chelating ligands containing sets of different donor atoms have been investigated.6,9–13 Some of these hybrid ligands have found important industrial applications, for instance the phosphinoenolates ([P,O] donors) used in the SHOP process.14–16 Combining two different donor atoms in a single ligand greatly expands the variety of catalyst structures available at a low synthetic cost and, at the same time, it offers the possibility of bringing together desirable features found in different types of catalysts. For example, Brookhart's nickel ethylene polymerization catalysts containing α-diimine nitrogen ligands7 are very active but have low thermal stability and are quite sensitive to impurities, while nickel phosphinoenolates are exceptionally robust oligomerization

catalysts. A ligand design combining key features of phosphinoenolates and α-diimines should produce a very active and stable polymerization catalyst. This seemingly ingenuous reasoning proves true in some cases; shortly after the discovery of α-diimine catalysts, Grubbs reported that nickel salicylaldiminate-based complexes containing imine and anionic phenolate fragments are very active olefin polymerization catalysts that tolerate polar impurities and can incorporate some types of functional monomers.17–19 These catalysts can perform ethylene polymerization even in aqueous emulsion, which undoubtedly constitutes an impressive achievement for a Ziegler–Natta related catalyst.20 Following the same line of thought, a large number of [P,N] ligands have been screened, with the aim of combining the exceptional properties of imine-based polymerization catalysts with the well-known stability of late transition metal phosphine complexes. Thus, nickel complexes with [P,N] ligands bearing bulky N-arylimino groups (phosphine-imine ligands) are very stable catalysts, which perform steadily at temperatures above 60 °C producing polyethylenes or heavy oligomer mixtures.21–23 Other nickel complexes with different [P,N] ligand designs containing nitrogen heterocycles as donor fragments, are very active ethylene oligomerization catalysts which produce mainly butenes and hexenes.24–33

Nickel catalysts with [P,N] ligands are usually generated from simple halide complexes by activation with organoaluminium derivatives. The choice of the co-catalyst (e.g., AlEtCl2, AlEt2Cl or alumoxane derivatives),23,27 and the catalyst/cocatalyst ratio are critical parameters which determine their activity and selectivity. In contrast, activation of the corresponding palladium complexes using aluminium cocatalysts appears to be inefficient, therefore they have seldom been reported.22,34 Very likely, one of the main causes for the dramatic influence of organoaluminium cocatalysts in these systems is their ability to attack sensitive organic functionalities present in the ligands.27 For example, they can remove acidic H atoms23 from enolizable [P,N] ligands,22,31 which leads to the formation of electrically neutral species. This is supported by the independent synthesis and isolation of complexes of anionic [P,N] enolates.35–37 Consequently, it has been shown that the activity and selectivity of the catalysts based on [P,N] ligands improves when these are non-enolizable.23 Another strategy to overcome problems associated to co-catalysts is to replace halide catalyst/aluminium cocatalyst systems by well-defined σ-alkyl complexes that do not require activation by organoaluminium compounds.38,39 A number of palladium methyl derivatives of the type [Pd(Me)(L')(P–N)]+ have been reported (where L' is a weakly coordinating ligand, usually MeCN) which oligomerize ethylene21,23,25,32,33,40–42 or copolymerize olefins and CO without cocatalysts.42–45 Although these systems are only moderately active, they provide a wealth of information on the mechanism of polymerization and copolymerization reactions, because they enabled the isolation of stable products arising from the migratory insertion of olefins and/or CO into the Pd–CH3 bond.23,41–48 These compounds can undergo unusual but potentially very interesting processes, such as the insertion of polar monomers.43,46,47 Therefore, it is rather surprising that analogous σ-alkyl or aryl complexes of nickel stabilized with [P,N] ligands have received very little attention as single-component catalysts. A few neutral σ-organonickel derivatives with anionic [P,N] ligands have been tested for this purpose, but in general they showed low catalytic activity.35,49–53

We recently described a series of Ni and Pd complexes bearing phosphinito-imines, a new type of non-enolizable [P,N] ligand that can be readily obtained from amides RCONHAr and chlorophosphines ClPR2.54 Similarly to related phosphine-imine complexes, Ni phosphinito-imine derivatives have become very active catalysts in the presence of organoaluminium cocatalysts (MMAO, ClAlEt2), while the corresponding Pd derivatives are inactive. Nickel catalysts produce mainly butenes with minor amounts of hexenes and octenes, which is surprising considering that these compounds are structurally analogous to phosphine-imine complexes that are ethylene polymerization catalysts. These results encouraged us to continue our work, synthesizing σ-alkyl complexes of Ni and Pd with phosphinito-imine ligands, which could undergo migratory insertion reactions into the metal–carbon bond, and possibly catalyze ethylene polymerization and/or copolymerization with carbon monoxide. For this purpose we resorted to facile ligand displacement reactions from the metallacycle complexes [M(CH$_2$CMe$_2$-*o*-C$_6$H$_4$)(L$_2$)] (M = Ni, L = pyridine (Py), 1a;55 M = Pd, L2 = 2,6-cyclooctadiene (cod), 1b56). These are very convenient precursors, significantly more stable than analogous open-chain dialkyl derivatives and readily prepared from simple starting materials.

Results and discussion

Synthesis of metallacyclic complexes

Phosphinito-imine ligands can be readily generated in situ as described previously.54 As shown in Scheme 1, ligand 2 is obtained by deprotonating N-(2,6-diisopropylphenyl)acetamide with n-BuLi, followed by treatment with chlorodiisopropylphosphine at −78 °C. The latter reaction produces 2 along with its phosphinoamide tautomer, 2′. Since the metallacycle fragment contained in the precursors 1 is not symmetric, it was foreseen that their reaction with the 2, 2′ mixture could produce up to four isomeric products. However treatment of the precursor nickel complex 1a with 2/2′ cleanly affords only two products, 3a and 3a′, characterized by sharp 31P signals at δ 188.2 and 185.9 ppm. The positions of these signals are not far from that of the complex [NiBr2(2)] (178.0 ppm), indicating that both 3a and 3a′ incorporate the ligand as the phosphinito-imine tautomer.54 Hence, the phosphinoamide tautomer 2′ rearranges upon coordination to the Ni center, as observed previously in the synthesis of [NiBr2(2)]. Their 1H and 13C NMR spectra show that 3a and 3a′ are cis/trans isomers

Monitoring the ligand exchange reaction by 31P NMR shows that the initial 3a/3a′ ratio is somewhat variable, ranging from ca. 1:1 to almost 3:1, depending on the experiment. Pure samples of the major isomer, 3a, can be isolated by careful recrystallization of the reaction mixture. Isomer 3a does not convert into 3a′ in solution at room temperature, therefore any conformational exchange is necessarily slow. In the 13C{1H} spectrum of 3a the characteristic signal of the metallacyclic CH2 at δ 57.5 ppm is split into a doublet with 2JCP = 72 Hz, while the coupling of the nickel-bound aromatic carbon (171.9 ppm) is only 8 Hz. This is a clear indication that the CH2 group is trans to the phosphorus atom. The second isomer, 3a′, was characterized as a mixture with 3a. As expected, the 13C resonances for the metal-bound carbons display the opposite carbon–phosphorus coupling pattern, with the larger coupling constant (98 Hz) corresponding to the quaternary aryl atom. In contrast with the conformational stability of 3a and 3a′, it was shown that the dihalide complex [NiBr2(2)] undergoes a fluxional process involving a tetrahedral, high-spin intermediate with a barrier of only 12.1 kcal mol−1.54 For 3a

and 3a', conformational inversion through a tetrahedral isomer is much more difficult because such intermediate is destabilized by the strongly σ-bound carbon ligand.

The reaction of the palladium metallacycle 1b with 2/2' produces a mixture of three products, originating resonances at δ 180.6, 175.6 and 110.8 ppm in the 31P{1H} NMR spectrum. The first two signals are in the same region as those of the phosphinito-imine complexes 3a/3a', therefore they can be assigned to the corresponding cis/trans pair of palladium metallacycles 3b/3b'. In most experiments, these are formed in an approximately constant 1.8:1 ratio. The amount of the third component, 4, varies widely from one experiment to another. Careful recrystallization of the mixture from hexane at −30 °C produced fractions of yellow and colorless crystals. The former contain isomers 3b/3b', and the latter correspond to pure compound 4. As expected, the NMR spectra of 3b/3b' closely resemble those of 3a/3a'. Similarly to their nickel analogues, the isomer with the higher field 31P resonance, 3b, corresponds to the isomer in which the CH2 group is placed in trans to P, as deduced from the 2JCP coupling constants measured in the 13C{1H} spectrum. Although 3b and 3b' could not be fully separated by fractional crystallization, samples with different isomer ratios were obtained that are stable in solution at room temperature. Thus, cis/trans exchange of the palladium phosphinito-imine metallacycles is also very slow or does not take place at room temperature.

The shielding of the 31P signal of 4 relative to those of 3b/3b' parallels the relationship between the chemical shifts of the free compound 2' (90 ppm) with regard to 2 (139 ppm). This strongly suggests that compound 4 contains phosphinoamide ligand instead of phosphinito-imine. In addition, the resonance due to the quaternary carbon atom of the 2,6-diisopropylphenyl in the 13C{1H} spectrum of 4 shows a carbon–phosphorus coupling of 6 Hz that is not observed in the spectra of phosphinito-imine complexes. This coupling, also observed in related complexes,57 points out the proximity of the nitrogen-bound carbon and the 31P nuclei and therefore can be regarded as a fingerprint for the phosphinoamide structure.

The 1H and 13C{1H} spectra of 4 show the characteristic signals of the metallacyclic fragment. The carbon resonances for the Pd-bound CH2 and quaternary aromatic carbon appear as doublets with respectively small (4 Hz) and large (123 Hz) 2JCP coupling constants, consistent with the CH2 and PR2 occupying mutually cis positions. This arrangement reflects the thermodynamic preference to place the weak σ-donor carbonyl group in trans to the CH2, which has a significantly stronger trans influence than the aryl group (antisymbiotic effect).58,59

The reaction of 1b with 2/2' is so far the only case in which we observed the coordination of phosphinito-imine and phosphinoamide tautomers. In this system, the phosphinito-imine is thermodynamically favored over the phosphinoamide, and therefore it is not surprising that the phosphinoamide ligand of 4 rearranges readily to phosphinito-imine. Such conversion is driven to completion when 4 is heated in THF solution at 60 °C for 5 h. Thus, the synthesis of the phosphinito–imine complexes 3b/3b' is best accomplished by heating the reaction mixture obtained from 1b and 2 once the ligand exchange has taken place, as described in the Experimental section. Interestingly, the 3b/3b' ratio obtained is always close to 1.8:1, which suggests that 3b is slightly thermodynamically favored over 3b'.

The identities of the Pd complexes 3b, 3b′ and 4 were confirmed on the basis of X-ray diffraction studies (Fig. 1–3). The structures of the phosphinito-imine complexes were determined from a single crystal containing 3b/3b′ isomers in 1:1 ratio. The three complexes exhibit slightly distorted square–planar structures. The metallacyclic fragment exhibits an "open envelope" folded conformation, also observed in related Pd cyclometallated neophyl derivatives.56 It is interesting to compare the lengths of the Pd–C bonds in the three complexes, since they reflect the different trans influence of the P, N and O donor atoms. Thus, on going from 3b to 3b′ the Pd–CH2 bond contracts from 2.081(3) Å to 2.049(3) Å, whilst the Pd–C(aryl) elongates from 2.008(3) to 2.076(3) Å, due to the stronger σ-donor capacity of P compared to N. However, this trend cannot be directly translated to the structure of 4. In this compound the Pd–C(aryl) bond is 2.0241(13) Å, significantly shorter than in 3b′, where the aryl group is also trans to the P donor. On the other hand, the Pd–CH2 bond length is nearly the same in both compounds, even though the imine group sitting in the trans position in 3b′ is a better σ-donor than the carbonyl of 4. This is probably due to the existence of significant steric repulsions between the close-by aryl fragments in 3b′, which are absent from 4 or 3b. In 3b′ these repulsions weaken the Pd–C(aryl) bond, but reinforce the other Pd–C interaction by a compensating effect. In line with this argument, the average of both Pd–C bonds decreases in the order 3b (2.061 Å) > 3b′ (2.046 Å) > 4 (2.033 Å), which suggests that the phosphinito-imine binds somewhat more strongly in 3b than in 3b′, while the phosphinoamide is a weaker ligand than phosphinito-imine, in spite of the steric effects. The almost strict planarity of the [P,N] chelate in 3b and 3b′ also suggests higher overall stability than the cycle formed by the [P,O] ligand in 4, which is puckered with a Pd–P–N–C12 torsion angle of 10.1°.

Protonation of metallacyclic complexes

Previous studies showed that protic acids selectively cleave the metal–aryl bond of nickel and palladium complexes containing the metallacyclic fragment M⌒(CH₂CMe₂-*o*-C₆⌒H₄), such as 3a or 3b, to afford the corresponding neophyl complexes.56,60 Reactive species with an open coordination site can be generated by using acids containing low coordination-capability anions, such as the tetraarylborate [H(OEt)2]+[BAr′4]− (Ar′ = 3,5-C6H3(CF3)2).61,62 As shown in Scheme 2, protonation of isomeric mixtures of phosphinito-imine complexes with [H(OEt)2]+[BAr′4]− proceeds cleanly under various conditions, affording cationic products that invariably exist as single isomers. This indicates that, in contrast with the parent metallacycles, these cationic monoalkyls isomerize readily to the thermodynamically favored isomer.

Treatment of the nickel metallacycles 3a/3a′ with [H(OEt)2]+[BAr′4]− produces a thermally unstable complex, 5, which can be isolated as a yellow precipitate when the reaction is carried out in hexane at −78 °C. Its 31P{1H} spectrum, recorded in CD2Cl2 at −40 °C, shows a single resonance at δ 193.4 ppm consistent with the presence of the phosphinito-imine ligand. The 1H and 13C{1H} spectra show signals corresponding to a coordinated molecule of diethyl ether, probably occupying the position trans to the phosphinito group. These signals are broad even at −80 °C, suggesting that the ether ligand is extremely labile, and experiences rapid intermolecular exchange. The fluxional process is responsible for the broadening of other signals in the spectrum, which prevents the unambiguous identification of the resonances

corresponding to the nickel-bound CH2 group. At 0 °C, the NMR spectra undergo irreversible changes due to the decomposition of the complex. In the 31P{1H} spectrum, the characteristic signal of 5 is cleanly replaced by a sharp resonance at δ 24 ppm. This splits into a doublet with a large coupling constant of 451 Hz when proton decoupling is turned off, denoting the presence of a hydrogen atom directly bound to P. The corresponding proton resonance is observed in the 1H spectrum as a wide doublet signal at δ 5.07 ppm, which is in good agreement with data reported for tertiary phosphonium salts.63 On the basis of its 1H and 13C{1H} spectra, this decomposition product was identified as the cation [HP(CH2CMe2Ph)(iPr2)]+. The assignment was confirmed by comparison of its NMR data (31P, 1H and 13C) with those of an authentic sample of the corresponding phosphonium tetrafluoroborate salt prepared by an independent method (see Experimental). Since no other decomposition products were detected,64 it is difficult to propose a mechanism for the breakdown process. However, very likely it involves the reductive C–P coupling of the phosphinite group and the alkyl chain as the initial stage.

Protonation of the palladium metallacycles 3b/3b' with [H(OEt)2]+[BAr'4]− leads to compound 6, which, in contrast with 5, is thermally stable in solution and resists exposure to air in the solid state for prolonged periods of time. The 31P{1H}, 1H and 13C{1H} NMR spectra of 6 clearly indicate the presence of the phosphinito-imine ligand and the palladium-bound alkyl fragment, but not diethyl ether nor any other auxiliary ligand. The CH2 group bound to Pd gives rise to a doublet at δ 16.6 ppm in the 13C{1H} spectrum with 2JPC = 7 Hz. The small value of the coupling constant denotes the cis arrangement of the strongly σ-donor phosphinito and alkyl ligands, as demanded by the antisymbiotic effect.61,62 Since the existence of a coordinative unsaturation of the Pd center would not be consistent with the robustness of the complex, it can be concluded that the metal center is stabilized by an intramolecular metal–arene π interaction. Such interaction is not rare for Pd(II) complexes.65–69 We reported before several examples of apparently unsaturated neophylpalladium complexes which exhibit intramolecular π,η1 or π,η2 coordination of the phenyl group.61,62 Arene π-coordination is bespoken by the upfield shift of the 13C resonances of the aromatic carbon atoms involved in the interaction. Although the resonance corresponding to the ipso carbon of the phenyl group is obscured by other signals in the densely populated aromatic region of the 13C spectrum, a signal at δ 119.4 ppm was unambiguously assigned to the ortho CH groups on the basis of the 1H and the 1H–13C HSQC heterocorrelation spectra. This signal is shifted by ca. 12 ppm to higher field from its normal position in neophyl derivatives. The chemical equivalence of the ortho and ortho' carbon atoms is maintained down to −75 °C, indicating that this π interaction is either symmetrical or that the Pd atom undergoes shifts between both ortho positions with a very low energy barrier.

The electrospray ionization (ESI) mass spectrum of 6 recorded from a diethylether solution is dominated by an intense signal for the cation molecular ion (m/z = 574) with the correct isotope pattern (Fig. 4). When this ion is isolated in the ion-trap analyzer and subsequently subjected to chemically induced fragmentation (CID), new peaks are observed with m/z = 518 and 440. These can be attributed to the successive neutral losses of isobutene (m = 44) and benzene (m = 78). Although 6 is indefinitely stable in condensed phase, the fragmentation pattern is strongly reminiscent of the spontaneous decomposition that the related neophyl derivative [Pd(σ:π-CH2CMe2Ph)(dmpe)]+ undergoes in solution. This process involves the

formation of an unstable phenylpalladium species via β-phenyl elimination, the inverse of migratory insertion.

In agreement with the solution NMR data, the crystal structure of compound 6 (Fig. 5) shows that the neophyl group acts as a bidentate ligand, with the σ Pd–CH2 bond and the π-bound phenyl groups occupying the cis and trans positions with regard to the P atom, respectively. Due to the low electron donor capacity of the arene, the trans Pd–P bond is unusually short, 2.1712(13) Å, nearly the same length as the Pd–N bond, 1.172(4) Å. The Pd–arene π interaction is characterized by very similar Pd–C3 (ipso) and Pd–C4 (ortho) distances, 2.491(5) and 2.463(5) Å respectively. The nearly symmetrical η2 coordination mode of the aromatic ring contrasts with the bonding in related Pd complexes containing intramolecular π-arene interactions, where the Pd–C (ipso) is always significantly shorter than the shortest of the two Pd–C (ortho) distances. A theoretical analysis concluded that these are best considered as η1-arene complexes, and that the interaction of the metal center with the ortho carbons has little relevance from the bonding point of view.66 The preference of 6 for η2 bonding is probably a consequence of the proximity of the N-aryl substituent of the imine functionality. As can be seen in the X-ray structure, the phenyl and 2,6-diisopropylphenyl aromatic rings arrange in almost parallel alignment suggesting the existence of attractive π-stacking forces between them. These forces could be responsible for a shift of the phenyl ring, bringing the metal center closer to the ortho carbon atom C4. In spite of being coordinated to the Pd atom, the C(3)–C(4) bond length is essentially unaltered and identical to that of the “free” C(3)–C(8) bond. This is consistent with the π-bond description as a ligand to metal electron donation, with little or no backdonation from the metal to the arene ring.

Due to the thermal instability of complex 5, we decided to prepare a more stable cationic nickel complex by replacing the diethyl ether molecule by a better donor acetonitrile ligand. Thus, complex 7a was prepared reacting 5 with an excess of acetonitrile. 7a is stable in solution at room temperature but it readily decomposes when warmed to 40 °C and similarly to 5, produces the phosphonium ion [HP(CH2CMe2Ph)(iPr)2]+. The palladium analogue, 7b, is also obtained when complex 6 is treated with acetonitrile.

The reactions described above enabled a qualitative assessment of the stability of π-arene interactions in Ni and Pd complexes. Since 6 is stable in diethyl ether solution but reacts with acetonitrile, it can be concluded that the internal π-arene linkage is weaker than a MeCN ligand, but it is stronger than Et2O. Although the nickel analogue of 6, the cation [Ni(σ:π-CH2CMe2Ph)(2)]+, could also exist (the related compound [Ni(σ:π-CH2CMe2Ph)(dtbpe)]+ was prepared and structurally characterized by Hillhouse and co-workers70), formation of the diethylether complex 5 is more favorable when the nickel metallacycles 3a/a’ react with the acid [H(OEt2)2][BAr’4], implying that the arene moiety binds more weakly to the Ni center than Et2O. Interestingly, both ions [M(CH2CMe2Ph)(2)]+ (M = Ni or Pd) are readily generated in the gas phase and observed in the ESI mass spectra of 7a and 7b. These spectra show no peaks for the corresponding molecular ions, but only for the ions resulting from acetonitrile loss. The ions observed in the spectra of 7b and 6 undergo identical sequences of neutral losses when subjected to CID fragmentation. The corresponding ion for 7a ([M]+ − CH3CN, m/z = 526) also exhibits the same fragmentation pattern, giving rise to the peaks resulting from successive isobutene and benzene losses (m/z = 470 and 393). This indicates that the structure of this nickel ion [Ni(CH2Me2Ph)(2)]+ is probably analogous to that of 6.

Compounds 7a and 7b are more readily prepared by reacting the metallacycles 3a/a' or 3b/b' with [H(OEt)2]+[BAr'4]− in acetonitrile. These compounds are characterized by single 31P resonances at 188.7 and 190.2 ppm, within the region of phosphinito-imine complexes. The presence of the acetonitrile ligand is substantiated by the observation of weak absorption bands at 2322 cm−1 in the IR spectra of both compounds.71 Their NMR spectra appear well resolved at room temperature, but some signals exhibit significant broadening which evidence that these compounds undergo fluxional processes that are different for each of them. Thus, broadening of the 1H and 13C resonances of the acetonitrile signals in the spectra of 7a point to intermolecular exchange of this ligand, as observed with diethylether for 5, while these signals appear sharp and well defined for 7b. On the other hand, the signal of ipso phenyl carbon of 7b is missing from its 13C spectrum, while the signal of the ortho shows an appreciable line broadening. Although this might be indicative of a reversible interaction of the phenyl with the Pd center, it is surprising that such process does not have a similar effect on the signals of acetonitrile, which would be competing for the same coordination position.

The crystal structures of the acetonitrile complexes 7a and 7b are shown in Fig. 6 and 7. These molecules display slightly distorted square-planar configurations with the stronger σ-donor PR2 and alkyl fragments sitting in mutually cis positions. In both molecules the phenyl ring is far removed from the metal center and therefore no π-interactions are present. Apart from the bond length differences due to the covalent radii of Ni and Pd, the only evident distinction between the two structures is the conformation adopted by the neophyl group. In the palladium complex, the CMe2Ph fragment is projected perpendicularly from the coordination plane, while in the Ni derivative, the Ni–C21 and C21–C22 bonds rotate to bring the phenyl group to a position roughly parallel to the vector defined by the acetonitrile ligand. This difference is probably caused by steric repulsions between the bulky CMe2Ph and P(iPr)2 fragments in the more congested environment of the nickel complex. It is worth noting that the Pd–P distance in 7b is ca. 0.02 Å longer than in 6, reflecting the stronger σ donor ability of MeCN compared to the arene.

Reactions of the cationic alkyl complexes with ethylene and CO

The cationic complexes 5, 6, 7a or 7b were unsuccessful as single-component catalysts for ethylene oligomerization/polymerization or the copolymerization of ethylene and CO. The lack of activity of the nickel derivatives could be explained on the basis of their thermal instability, as even the stabilized acetonitrile adduct decomposes under mild conditions. The fact that decomposition of the nickel cationic alkyls involves the cleavage of the phosphinito-imine ligand and the formation of tertiary phosphonium salts suggests that the previously reported catalysts for ethylene oligomerization catalysts generated from nickel phosphinito-imine dihalide complexes and organoaluminum co-catalysts could actually involve a simple nickel containing a tertiary phosphane ligand.54

Introducing a large excess of ethylene to a CD2Cl2 solution of 6 at room temperature and atmospheric pressure does not alter significantly its NMR spectra, indicating that ethylene does not displace readily the intramolecular Pd–arene interaction. Although our data does not rule out the possibility that a small amount of the alkyl–ethylene complex is formed under

these conditions, the subsequent migratory insertion step is probably unfavorable. Brookhart has shown that the energy barrier for ethylene insertion into a Pd–C bond is considerably higher for complexes containing hybrid P,N ligands (ca. 19–25 kcal mol−1) than for related complexes containing symmetrical diphosphine or diimine ligands (ca. 17 kcal mol−1).23,31 The failure of palladium phosphinito–imine complexes to catalyze CO/ethylene copolymerization is more surprising, since several Pd complexes containing closely related phosphine–imine ligands are able to catalyze this reaction.42–48 Therefore, we decided to investigate the reactions of complexes 6, 7a and 7b with carbon monoxide.

The carbonylation reactions of complexes 7a and 7b proceed in a straightforward manner affording the corresponding acyl complexes, which were isolated in good yield (Scheme 3). The nickel derivative 7a reacts rapidly at room temperature with 1 atm. of CO yielding the acyl complex 8a, characterized by a 31P resonance at δ 181.4 ppm. The IR spectrum of this compound has three absorption bands at 1625, 1709 and 2321 cm−1, assigned to the C═N (imine), C═O (acyl), and C≡≡N (nitrile) stretch vibrations. The presence of the acyl fragment is also supported by the 13C{1H} spectrum, which shows the carbonyl resonance at δ 241.5 ppm as a doublet due to the coupling to phosphorus. The 2JCP coupling constant, 20 Hz, is consistent with the cis arrangement of the acyl relative to the phosphinite group, as shown in Scheme 3. The ESI spectrum of 8a does not show the expected ion peak at m/z 595 amu, but, two ion clusters with peaks at 554 and 526 amu resulting from the loss of acetonitrile and acetonitrile and CO, respectively. This is not surprising considering that CO insertion is generally reversible. The tendency of 8a to decarbonylate was confirmed when a dichloromethane solution of this compound in a septum-capped NMR tube was heated at 40 °C and monitored by 31P NMR. After 3 days, the resonance of 8a fully disappears and was replaced by two new peaks at δ 188 and 24 ppm, corresponding to 7a and to the phosphonium product arising from its decomposition.

The palladium alkyl complex 7b also reacts with CO, but with considerably more difficulty than its nickel counterpart. The reaction does not take place in dichloromethane solution under the ambient conditions. Full conversion to the acyl complex 8b could be achieved after stirring under 4 bar of CO for 1 h. The spectroscopic features of this acyl derivative are similar to those of 8a. Thus, the IR absorptions for the C═N, C═O and C≡≡N stretches appear at 1638, 1728 and 2320 cm−1, respectively, and the acyl carbon gives rise to a doublet at δ 219.9 ppm in the 13C{1H} spectrum with 2JCP = 20 Hz. 8b also decarbonylates in the gas phase, but its ESI spectrum only shows a single ion with m/z = 574 amu, corresponding to the loss of acetonitrile and CO. Nevertheless, 8b is very stable in solution up to 60 °C, which is in contrast with the low stability of many cationic palladium acyl complexes either in solution or in the solid state.72–76Fig. 8 shows the crystal structure of compound 8b. As can be seen, the acyl functionality is oriented almost perpendicularly to the mean coordination plane, forming an angle of 114.3°, while the neophyl fragment adopts approximately the same configuration as in the precursor complex 7b.

In contrast to the nitrile complexes 8, the π-arene derivative 6 was recovered unaltered after treatment with CO. As already mentioned, this compound does not catalyze ethylene/CO copolymerization either. However, when exposed to 6 bar of a 1:1 CO/ethylene mixture at 60 °C, it cleanly reacts giving rise to a new product, 9, isolated as a colorless crystalline solid in

>60% yield after recrystallization. The crystal structure of this compound (Fig. 9) displays a five-membered metallacycle arising from the consecutive insertions of CO and ethylene into the Pd–CH2 bond. Its spectroscopic features are in good agreement with the solid-state structure. For example, the 13C{1H} spectrum shows a singlet at δ 253.6 ppm attributed to the carbonyl carbon, while the ethylene fragment gives rise to two triplets at δ 1.56 and 2.67 ppm in the 1H spectrum. The ESI spectrum shows a peak cluster at m/z = 630 corresponding to the molecular ion. CID fragmentation of this ion causes the simultaneous loss of ethylene and CO, affording the [Pd(CH2CMe2Ph)(2)]+ ion (m/z = 533), which subsequently eliminates isobutene (m/z = 517) and benzene (m/z = 440), as previously observed in the spectra of 6 and 7b.

The formation of complex 9 demonstrates that the lack of reactivity of 6 towards CO is only apparent, since the formation of an acyl species must precede the ethylene insertion. In order to detect such species, the reactivity of 6 towards CO was investigated in situ with variable temperature NMR. Using a thick-walled NMR tube, the 31P, 1H and 13C NMR spectra of 6 were recorded under a pressure of 4 bar of CO. At −20 °C, the 31P{1H} spectrum shows a main signal at 170.0 ppm and a minor peak at 185.6 ppm in ca. 7:1 ratio. The 13C{1H} spectrum of the main species displays a resonance at 215.6 ppm that is consistent with the presence of an acyl ligand, and is similar to the corresponding signal of the acetonitrile acyl complex 8b (219.9 ppm). The deshielding of the signal for the neophyl CH2 group, at 73.2 ppm, further supports CO insertion. All signals in the phenyl region are in their normal positions, indicating that the π arene interaction is displaced, probably by a CO ligand. Evidence for the presence of a carbonyl ligand was obtained by treating 6 with 13CO. Due to the limited availability of this reagent, 13CO was bubbled at normal pressure through a CD2Cl2 solution of 6 at −60 °C and NMR spectra were recorded at this temperature. Under these conditions, three signals in 2:1:7 ratio were observed in the 31P{1H} spectrum at 186.6, 185.2 and 169.8 ppm, the latter corresponding to the major species detected in the former experiment. The signals at 169.8 and 186.2 ppm are split in doublets with 2JCP coupling constants of 114 and 80 Hz, respectively, both of them consistent with a trans coordination of carbonyl to the P atom. The singlet at 185.2 ppm corresponds to a small amount of unreacted 6. According to these data, the major species is the acyl–carbonyl complex [Pd(COCH2CMe2Ph)(CO)(P–N)]+, 11, and the peak for the minor species at 186.6 ppm corresponds to the carbonyl derivative [Pd(CH2CMe2Ph)(CO)(P–N)]+, 10. The carbonyl resonances for these compounds are observed in the 13C{1H} spectrum as doublets at δ 175.6 and 172.6 ppm, respectively.

Complexes 10 and 11 are formed in chemical equilibrium. As expected, the acyl species is favored at low temperature. Under a CO pressure of 4 bar the intensity ratio of the 31P resonances of 11 and 10 gradually decreases from 7:1 at −20 °C to ca. 1:1 at 30 °C. At −20 °C, the 1H spectrum of alkyl 10 is appreciably broadened, suggesting that rapid dissociative exchange of CO might be taking place, with the formation of small amounts of 6. Under these conditions, the signals of 11 appear sharp and well resolved, because CO de-insertion is a much slower process. These observations enable us to draw the mechanistic picture for the formation of complex 9 from 6 illustrated in Scheme 4. Noteworthy, although the CO ligand of 11 is less labile than in 10, only the former is reactive enough to undergo ethylene insertion.

Chelate species similar to 9 are important intermediates in the palladium-catalyzed alternating copolymerization of ethylene and CO.6,8,77,78 In general, these complexes are unstable, although a number of them have been isolated and characterized.42,77–82 Hybrid P,N43–48 or P,O83 ligands increase the stability of these compounds, but also decrease their reactivity, preventing the progress of the copolymerization reaction.

Conclusions

A series of σ-organonickel and -palladium complexes stabilized by phosphinito-imine ligands have been synthesized and fully characterized. Metallacyclic complexes 3 are readily available through ligand exchange from the suitable precursors directly using in situ generated mixtures of phosphinito-imine ligand and its amidophosphine tautomer. The coordinated amidophosphine tautomer rearranges to the phosphinito-imine form. This rearrangement is very fast for nickel complexes, but the palladium amidophosphine complex, 4, is stable enough to be isolated and characterized. Metallacycles 3a/b react with complete regioselectivity with protic acids, which made the synthesis of several cationic alkyl derivatives possible. These cationic alkyls are obtained exclusively as the thermodynamically more favorable isomer, in which the strongly σ-donor P and C ligands avoid occupying mutually trans positions. This implies that cis/trans isomerization of the less stable isomer is not only feasible but a facile process.

Cationic alkylnickel phosphinito-imine complexes are thermally sensitive, spontaneously undergoing a decomposition process involving the breakdown of the phosphinito-imine ligand and formation of the phosphonium ion [HP(iPr)2(CH2CMe2Ph)]+. However, the analogous Pd complexes are much more stable. Compound 6, a base-free complex stabilized by an intramolecular π-arene interaction is surprisingly robust. ESI mass spectra of the cationic nickel complexes showed that the analogous base-free nickel species can also be generated in the gas phase.

Disappointingly, cationic alkyl phosphinito-imine complexes are not active as single-component catalysts for olefin polymerization or copolymerization reactions. However, these compounds readily undergo migratory insertion of CO to give the corresponding acyls, and complex 6 reacts consecutively with CO and ethylene, quantitatively affording a very stable chelate derivative, 9. Lack of catalytic activity could be ascribed to thermal instability in the case of the nickel complexes, but not so for the much more stable palladium derivatives. For the latter, the lack of reactivity towards ethylene, and the high stability of 9 are the reasons. As pointed out by Brookhart,21,39 the strongly disparate donor capabilities of the PR2 and imine groups of the PN ligand stabilize these compounds, hence increasing the energy barrier for migratory insertion. Nevertheless, the ability of both nickel and palladium alkyls to undergo the cis/trans isomerization suggests that more reactive species should be accessible during hypothetical olefin polymerization or copolymerization process. Thus, similar cationic σ-alkyl complexes of nickel and palladium stabilized by other [P,N] ligands could prove catalytically active complexes. We are currently exploring various alternatives along this line of research.

Experimental section

General considerations

All experiments were carried out under dry nitrogen using standard Schlenk techniques. Solvents were rigorously dried and degassed before use. Microanalyses were performed by the Analytical Service of the Instituto de Investigaciones Químicas (Sevilla, Spain). Infrared spectra were recorded on a Bruker Vector 22 spectrometer, and NMR spectra on Bruker DRX 400 and 500 MHz and Bruker DPX 300 MHz spectrometers. The 1H and 13C{1H} NMR resonances of the solvent were used as the internal standard, but the chemical shifts are reported with respect to TMS. Assignation of the resonances was routinely aided by using gated 13C, 2D homonuclear H–H COSY and phase-sensitive NOESY spectra, and binuclear 13C–1H HSQC heterocorrelations. 31P NMR resonances are referenced to external 85% H3PO4. Compounds H(OEt2)2BAr'4,84N(2,6-iPr2C6H3)C(O)Me,85 [Ni⎡⎤(CH$_2$CMe$_2$-*o*-C$_6$⎡⎤H$_4$)(Py$_2$)] (**1a**)[55] and [Pd⎡⎤(CH$_2$CMe$_2$-*o*-C$_6$⎡⎤H$_4$)(cod)] (1b)56 were prepared as reported previously. Ligand 2 was generated in solution and used in situ as described before.54

Synthesis of 3a/3a'. A THF solution of ligand 2/2' (1.2 mmol) prepared in situ as described above was added to a solution of 1a (420 mg, 1.2 mmol) in 10 mL of THF at −78 °C. The reaction mixture was allowed to warm to room temperature while stirred. After 30 min, the solvent was evaporated under vacuum, and the orange residue was extracted with 40 mL of hexane and filtered through Celite. The extract contains a mixture of isomers 3a and 3a'. The solution was concentrated and cooled to −10 °C to afford compound 3a as an orange solid. Yield: 68% (0.43 g). Anal. Calcd for C30H46NNiOP: C, 68.46; H, 8.81; N, 2.66. Found: C, 67.79; H, 8.68; N, 2.77. IR (Nujol mull): v(CN) 1606 cm−1. 3a: 1H NMR (25 °C, C6D6, 300 MHz): δ 0.96 (d, 6H, 3JHH = 7 Hz, N{(CHMe2)2C6H3}), 1.15 (dd, 6H, 3JHH = 7 Hz, 3JHP = 2 Hz, PCHMe2), 1.19 (dd, 6H, 3JHH = 7 Hz, 3JHP = 3 Hz, PCHMe2), 1.22 (s, 3H, MeC(O)N), 1.40 (d, 6H, 3JHH = 7 Hz, N{(CHMe2)2C6H3}), 1.57 (s, 6H, CMe2), 1.61 (d, 2H, 3JHP = 5 Hz, CH2), 2.02 (m, 2H, PCHMe2), 3.26 (h, 2H, 3JHH = 7 Hz, N{(CHMe2)2C6H3}), 6.98–7.09 (m, 4H, o-C6H4), 7.13–7.18 (m, 3H, N{(CHMe2)2C6H3}). 13C{1H} NMR (25 °C, C6D6, 75 MHz): δ 16.7 (d, 2JCP = 8 Hz, PCHMe2), 17.8 (d, 2JCP = 9 Hz, PCHMe2), 18.4 (s, MeC(O)N), 23.7 (s, N{(CHMe2)2C6H3}), 24.1 (s, N{(CHMe2)2C6H3}), 28.1 (d, 1JCP = 7 Hz, PCHMe2), 28.6 (s, N{(CHMe2)2C6H3}), 34.2 (d, 4JCP = 5 Hz, CMe2), 47.9 (d, 3JCP = 5 Hz, CMe2), 56.8 (d, 2JCP = 76 Hz, CH2), 121.8 (s, CHar, o-C6H4), 122.8 (s, CHar, o-C6H4), 122.9 (d, 4JCP = 3 Hz, CHar, o-C6H4), 123.8 (s, m-CHar, N-Ar), 126.4 (s, N{(CHMe2)2C6H3}: p-CHar, N-Ar), 140.7 (s, o-Car, N-Ar), 142.1 (d, 3JCP = 4 Hz, ipso-Car, N-Ar), 143.6 (d, 3JCP = 7 Hz, CHar, o-C6H4), 155.4 (d, 3JCP = 8 Hz, Car, o-C6H4), 170.6 (d, 2JCP = 8 Hz, MeC(O)N), 171.9 (d, 2JCP = 8 Hz, Ni-Car). 31P{1H} NMR (25 °C, C6D6, 121.5 MHz): δ 185.9 (s). Mixture of3aand3a': 1H NMR (25 °C, CD2Cl2, 300 MHz): δ 0.96 (d, 3JHH = 2 Hz, N{(CHMe2)2C6H3}, 3a'), 0.96 (s, CMe2, 3a'), 1.00 (m, CH2, 3a'), 1.10 (m, CH2, 3a), 1.12 (m, N{(CHMe2)2C6H3},3a + 3a'), 1.28 (s, CMe2, 3a), 1.35 (d, 3JHH = 7 Hz, N{(CHMe2)2C6H3}, 3a), 1.43 (m, PCHMe2, 3a + 3a'), 1.81 (s, MeC(O)N, 3a), 1.83 (m, PCHMe2, 3a + 3a'), 1.85 (s, MeC(O)N, 3a'), 2.43 (m, PCHMe2, 3a + 3a'), 3.18 (m, N{(CHMe2)2C6H3}, 3a + 3a'), 5.45 (t, 3JHH = 6 Hz, CHar, o-C6H4, 3a'), 6.20 (t, 3JHH = 7 Hz, CHar, o-C6H4, 3a'), 6.50–6.70 (m, o-C6H4, 3a + 3a'), 6.76 (t, 3JHH = 7 Hz, CHar, o-C6H4, 3a), 6.97 (d, 3JHH = 7 Hz, CHar, o-C6H4, 3a), 7.10–7.30 (m, N-Ar, 3a + 3a'). 31P{1H} NMR (25 °C, CD2Cl2, 121 MHz): δ 185.9 (s, trans isomer), 188.2 (s, cis isomer). 13C{1H} NMR (25 °C, CD2Cl2, 75 MHz) (data for 3a' only): δ 16.7 (s, PCHMe2), 17.2 (d, 2JCP = 7 Hz, PCHMe2), 17.4 (s, MeC(O)N), 22.8 (s, N{(CHMe2)2C6H3}), 23.4 (s, N{(CHMe2)2C6H3}), 27.2 (d, 1JCP = 13 Hz, PCHMe2), 28.9 (s, N{(CHMe2)2C6H3}), 31.2 (d, 2JCP = 17 Hz, CH2), 34.5 (s, CMe2), 50.5 (d, 3JCP = 10 Hz, CMe2), 120.2 (s, CHar, o-C6H4), 121.9 (s,

CHar, o-C6H4), 122.7 (s, CHar, o-C6H4), 123.9 (s, m-CHar, N-Ar), 126.5 (s, p-CHar, N-Ar), 135.4 (d, 3JCP = 6 Hz, CHar, o-C6H4), 140.7 (s, o-Car, N-Ar), 143.1 (d, 3JCP = 3 Hz, ipso-Car, N-Ar), 166.1 (d, 3JCP = 3 Hz, Car, o-C6H4), 168.0 (d, 2JCP = 98 Hz, Ni-Car), 170.1 (d, 2JCP = 7 Hz, MeC(O)N).

Synthesis of 3b and 3b'. 20 mL of a THF solution of ligands 2/2' (2 mmol) prepared in situ as described above was added at −78 °C to a solution of 1b (692 mg, 2 mmol) in 15 mL of THF. The reaction mixture was heated at 60 °C for 5 h. The solvent was evaporated under vacuum and the yellow residue was extracted with 60 mL of hexane and filtered through Celite. The solution was taken to dryness and the residue was recrystallized from hexane at −10 °C to yield 3b/3b' as yellow crystals in 64% yield (0.73 g). Anal. Calcd for C30H46NOPPd: C, 62.76; H, 8.08; N, 2.44. Found: C, 62.42; H, 7.86; N, 2.37. IR (Nujol mull): ν(C═N) 1623 cm−1. 1H NMR (25 °C, C6D6, 300 MHz): δ 1.05 (d, 3JHH = 7 Hz, N{(CHMe2)2C6H3}, 3b'), 1.10–1.20 (N{(CHMe2)2C6H3}, PCHMe2, 3b + 3b'), 1.12 (CMe2, 3b + 3b'), 1.30 (d, 3JHH = 8 Hz, N{(CHMe2)2C6H3}, 3b), 1.39 (obscured signal, CH2, 3b), 1.91 (s, MeC(O)N, 3b), 1.94 (s, MeC(O)N, 3b'), 2.11 (d, 3JHP = 10 Hz, CH2, 3b'), 2.30–2.50 (PCHMe2, 3b + 3b'), 3.07 (m, N{(CHMe2)2C6H3}, 3b + 3b'), 5.51 (t, 3JHH = 8 Hz, CHar, o-C6H4, 3b'), 6.31 (t, 3JHH = 7 Hz, CHar, o-C6H4, 3b'), 6.60–6.80 (m, CH2CMe2-o-C6H4, 3b + 3b'), 6.82 (t, 3JHH = 8 Hz, CHar, o-C6H4, 3b), 7.10–7.30 (m, CHar, N-Ar, 3b + 3b'), 7.14 (d, 3JHH = 8 Hz, o-C6H4, 3b + 3b'). 13C{1H} NMR (25 °C, C6D6, 75 MHz): δ 16.5 (s, PCHMe2, 3b), 16.6 (s, PCHMe2, 3b'), 17.1 (d, 2JCP = 11 Hz, PCHMe2, 3b'), 17.1 (s, MeC(O)N, 3b'), 17.5 (d, 2JCP = 17 Hz, PCHMe2, 3b), 17.6 (s, MeC(O)N, 3b), 22.9 (s, N{(CHMe2)2C6H3}, 3b'), 23.4 (s, N{(CHMe2)2C6H3}, 3b'), 23.5 (s, N{(CHMe2)2C6H3}, 3b), 23.8 (s, N{(CHMe2)2C6H3}, 3b), 28.2 (d, 1JCP = 10 Hz, PCHMe2, 3b'), 28.3 (d, 1JCP = 4 Hz, PCHMe2, 3b), 28.5 (s, N{(CHMe2)2C6H3}, 3b), 28.6 (s, N{(CHMe2)2C6H3}, 3b'), 34.4 (d, 4JCP = 3 Hz, CMe2, 3b), 34.5 (s, CMe2, 3b'), 35.4 (d, 2JCP = 5 Hz, CH2, 3b'), 48.2 (d, 3JCP = 6 Hz, CMe2, 3b), 50.4 (d, 3JCP = 7 Hz, CMe2, 3b'), 57.4 (d, 2JCP = 100 Hz, CH2, 3b), 120.9 (d, 4JCP = 3 Hz, CHar, o-C6H4, 3b'), 122.6 (s, CHar, o-C6H4, 3b'), 122.7 (s, CHar, o-C6H4, 3b), 123.0 (s, CHar, o-C6H4, 3b), 123.1 (s, CHar, o-C6H4, 3b'), 123.7 (s, CHar, o-C6H4, 3b), 123.9 (s, m-CHar, N-Ar, 3b), 124.0 (s, m-CHar, N-Ar, 3b'), 126.2 (s, p-CHar, N-Ar, 3b'), 126.4 (s, p-CHar, N-Ar, 3b), 133.9 (d, 3JCP = 7 Hz, CHar, o-C6H4, 3b'), 140.1 (s, o-Car, N-Ar, 3b), 140.2 (s, o-Car, N-Ar, 3b'), 141.8 (s, ipso-Car, N-Ar, 3b), 142.6 (s, ipso-Car, N-Ar, 3b'), 142.6 (d, 3JCP = 14 Hz, CHar, o-C6H4, 3b), 158.0 (d, 2JCP = 8 Hz, Car, o-C6H4, 3b), 165.0 (d, 3JCP = 2 Hz, Car, o-C6H4, 3b'), 169.8 (s, MeC(O)N, 3b'), 170.1 (s, MeC(O)N, 3b), 171.0 (d, 2JCP = 8 Hz, Pd-Car, 3b), 171.9 (d, 2JCP = 143 Hz, Pd-Car, 3b'). 31P{1H} NMR (25 °C, C6D6, 121 MHz): δ 175.6 (s, 3b), 180.6 (s, 3b').

Compound 4. Colorless crystals of this compound grew from hexane at −10 °C when the reaction mixture obtained as described above was not heated at 60 °C. Anal. Calcd for C30H46Cl2NOPPd·1/2 C6H14: C, 64.22; H, 8.66; N, 2.27. Found: C, 63.96; H, 8.34; N, 2.36. IR (Nujol mull): ν(C═O) 1601 cm−1. 1H NMR (25 °C, C6D6, 300 MHz): δ 0.62 (dd, 6H, 3JHH = 7 Hz, 3JHP = 14 Hz, PCHMe2), 0.77 (d, 6H, 3JHH = 7 Hz, N{(CHMe2)2C6H3}), 1.03 (d, 6H, 3JHH = 7 Hz, N{(CHMe2)2C6H3}), 1.36 (dd, 6H, 3JHH = 7 Hz, 3JHP = 19 Hz, PCHMe2), 1.40 (s, 3H, MeC(O)N), 1.77 (s, 6H, CMe2), 1.94 (m, 2H, PCHMe2), 2.81 (h, 2H, 3JHH = 7 Hz, N{(CHMe2)2C6H3}), 2.94 (d, 2H, 3JHP = 5 Hz, CH2), 6.84 (d, 2H, 3JHH = 8 Hz, m-CHar, N-Ar), 7.01 (t, 1H, 3JHH = 8 Hz, p-CHar, N-Ar), 7.27 (d, 1H, 3JHH = 8 Hz, CHar, o-C6H4), 7.32 (d, 1H, 3JHH = 7 Hz, CHar, o-C6H4), 7.37 (m, 1H, CHar, o-C6H4), 8.48 (t, 1H, 3JHH = 7 Hz, CHar, o-C6H4). 13C{1H} NMR (25 °C,

C6D6, 75 MHz): δ 16.2 (d, 2JCP = 4 Hz, PCHMe2), 20.8 (d, 2JCP = 16 Hz, PCHMe2), 22.9 (s, MeC(O)N), 23.5 (s, N{(CHMe2)2C6H3}), 24.9 (s, N{(CHMe2)2C6H3}), 26.4 (d, 1JCP = 4 Hz, PCHMe2), 28.3 (s, N{(CHMe2)2C6H3}), 34.2 (s, CMe2), 38.6 (d, 2JCP = 4 Hz, CH2), 51.0 (d, 3JCP = 7 Hz, CMe2), 121.9 (d, 4JCP = 4 Hz, CHar, o-C6H4), 123.9 (d, 3JCP = 7 Hz, CHar, o-C6H4), 124.2 (s, CHar, o-C6H4), 125.3 (s, N{(CHMe2)2C6H3}: mCHar), 129.6 (s, p-CHar, N-Ar), 135.2 (d, 2JCP = 6 Hz, ipso-Car, N-Ar), 146.4 (s, o-Car, N-Ar), 164.6 (s, Car, o-C6H4), 170.2 (d, 2JCP = 123 Hz, Pd-Car), 181.7 (d, 2JCP = 16 Hz, MeC(O)N). 31P{1H} NMR (25 °C, C6D6, 121 MHz): δ 110.8 (s).

Synthesis of compound 5. 20 mL of a hexane solution of compounds 3a/3a' (274 mg, 0.52 mmol) cooled at −78 °C were added to a stirred suspension of 524 mg (0.52 mmol) of H(Et2O)2BAr'4 in 10 mL of hexane at −78 °C, causing immediate precipitation of a yellow solid. After 30 min of stirring at this temperature, the solution was filtered and the solid was rinsed with hexane (3 × 10 mL) at −50 °C. The product was dried under vacuum, keeping the temperature below −40 °C. Yield: 84% (0.64 g). The thermal instability of compound 5 prevented a satisfactory elemental analysis. 1H NMR (−40 °C, CD2Cl2, 300 MHz): δ 0.82 (d, 6H, 3JHH = 7 Hz, N{(CHMe2)2C6H3}), 1.04 (d, 6H, 3JHH = 7 Hz, N{(CHMe2)2C6H3}), 1.10 (m, 6H, PCHMe2), 1.10 (bs, 6H, (CH3CH2)2O), 1.41 (s, 6H, CMe2), 1.47 (bm, 6H, PCHMe2), 1.78 (s, 3H, MeC(O)N), 2.37 (bm, 2H, PCHMe2), 2.88 (bm, 2H, N{(CHMe2)2C6H3}), 3.43 (bs, 4H, (CH3CH2)2O), 7.13 (d, 2H, 3JHH = 7 Hz, o-CHar, N-Ar), 7.18–7.38 (m, 5H, o-C6H4 and N-Ar), 7.40 (d, 1H, 3JHH = 7 Hz, o-CHar, o-C6H4), 7.48 (s, 4H, BAr'4), 7.64 (s, 8H, BAr'4). 13C{1H} NMR (−40 °C, CD2Cl2, 75 MHz): δ 15.5 (s, (CH3CH2)2O), 16.5 (s, PCHMe2), 17.0 (s, MeC(O)N), 17.5 (s, PCHMe2), 17.5 (s, N{(CHMe2)2C6H3}), 28.0 (d, 1JCP = 25 Hz, PCHMe2), 29.1 (s, N{(CHMe2)2C6H3}), 34.0 (s, CMe2), 39.9 (s, CMe2), 66.4 (s, (CH3CH2)2O), 117.4 (s, p-CHar, BAr'4), 125.0 (q, 1JCF = 272 Hz, CF3 BAr'4), 125.2 (s, m-CHar, N-Ar), 126.0 (s, o-CHar, o-C6H4), 127.7 (s, p-CHar, N-Ar), 127.8 (s, p-CHar, o-C6H4), 128.9 (s, m-CHar, o-C6H4), 129.3 (q, 2JCF = 31 Hz, CF3-Car, BAr'4), 133.2 (s, ipso-Car, N-Ar), 135.2 (s, o-CHar, BAr'4), 141.1 (s, o-Car, N-Ar), 150.5 (bs, Ni-Car), 166.2 (q, 1JCB = 50 Hz, B-Car), 171.2 (s, MeC(O)N). 31P{1H} NMR (−40 °C, CD2Cl2, 121 MHz): δ 193.4 (bs).

Decomposition of compound 5 and synthesis of [HP(iPr2)2(CH2CMe2Ph)][BF4]. A solution of complex 5 in CD2Cl2 was allowed to warm from −40 °C to 0 °C in the NMR probe, and NMR spectra were recorded. The signals of 5 disappear and are replaced by those for the phosphonium cation [HP(iPr2)2(CH2CMe2Ph)]+. The assignation was confirmed by comparison with an authentic sample of the cation as the BF4− salt, which was prepared as follows: 1 mL (6.2 mmol) of PiPr2Cl was added to a stirred solution of neophylmagnesium chloride (7.8 mmol) in 60 mL of diethyl ether at −40 °C. The stirring was continued at room temperature for 24 h. After this time, the mixture was quenched with 50 mL of a saturated aqueous solution of NH4Cl. The organic layer was separated, dried over Na2SO4 and filtered. An ethereal solution of HBF4 was added at room temperature, and the product precipitated as a white solid. The mixture was allowed to stand for 12 h, the solid was collected by filtration and dried under vacuum. Anal. Calcd for C16H28BF4P: C, 56.38; H, 8.35. Found: C, 56.84; H, 8.21. 1H NMR (25 °C, CD2Cl2, 300 MHz): δ 1.17 (dd, 6H, 3JHP = 18.9 Hz, 3JHP = 7.2 Hz, PCHMe2), 1.20 (dd, 6H, 3JHP = 18.6 Hz, 3JHP = 7.2 Hz, PCHMe2), 1.63 (d, 6H, 4JHP = 1.7 Hz, CMe2), 2.23 (m, 2H, PCHMe2), 2.53 (dd, 2H, 2JHP = 11.5 Hz, 3JHH = 4.8 Hz, CH2), 5.64 (dm, 1H, 1JHP = 467 Hz, HP), 7.32 (t, 1H, 3JHH = 7.3 Hz, p-CHar, Ph), 7.43 (t, 2H, 3JHH = 8.1 Hz, m-CHar, Ph), 7.50 (d, 2H, 3JHH = 7.7 Hz, o-CHar). 13C{1H} NMR (25 °C, CD2Cl2, 100 MHz): δ 16.8 (s, PCHMe2), 16.9 (s,

PCHMe2), 20.3 (d, 1JCP = 42 Hz, PCHMe2), 29.2 (d, 1JCP = 42 Hz, CH2), 29.7 (d, 3JCP = 8 Hz, CMe2), 37.1 (d, 2JCP = 5 Hz, CMe2), 126.3 (s, o-CHar, Ph), 128.2 (s, p-CHar, Ph), 129.6 (s, m-CHar, Ph), 144.7 (s, ipso-Car, Ph). 31P{1H} NMR (CD2Cl2, 121 MHz): δ 22.9.

Synthesis of complex 6. A solution of 354 mg (0.35 mmol) of H(Et2O)2BAr'4 in 5 mL of dichloromethane was added to 201 mg (0.35 mmol) of isomers 3b/3b' dissolved in 10 mL of dichloromethane at −78 °C. The reaction mixture was allowed to warm to room temperature while stirred. After 30 min, solvent was removed under reduced pressure, and the residue was rinsed with 10 mL of hexane, extracted with 20 mL of ether and filtered. The solution was taken to dryness, and the residue was recrystallized from a 2:1 ether:hexane mixture affording 6 as colorless needles. Yield: 64% (0.34 g). Anal. Calcd for C62H59BF24NOPPd: C, 51.73; H, 4.10; N, 0.97. Found: C, 51.73; H, 4.05; N, 1.11. IR (Nujol mull): ν(C═N) 1626 cm−1. ESI-MS from Et2O: m/z 574.2 (M+). CID fragmentation of ion m/z 574.2: m/z 518.1 (M+ − CH2CMe2), 440.1 (M+ − CH2CMe2Ph). 1H NMR (−20 °C, CD2Cl2, 300 MHz): δ 0.95 (d, 6H, 3JHH = 7 Hz, N{(CHMe2)2C6H3}), 1.22 (bd, N{(CHMe2)2C6H3}), 1.26 (dd, 6H, 3JHH = 7 Hz, 3JHP = 5 Hz, PCHMe2), 1.33 (bm, 6H, PCHMe2), 1.33 (s, 6H, CMe2), 1.40 (d, 2H, 3JHP = 5 Hz, CH2), 1.81 (s, 3H, MeC(O)N), 2.32 (h, 2H, 3JHH = 7 Hz, N{(CHMe2)2C6H3}), 2.48 (m, 2H, PCHMe2), 6.45 (t, 1H, 3JHH = 8 Hz, p-CHar, Ph), 7.03 (t, 2H, 3JHH = 8 Hz, m-CHar, Ph), 7.14–7.24 (m, 3H, N-Ar), 7.48 (s, 4H, BAr'4), 7.52 (d, 2H, 3JHH = 7 Hz, o-CHar, Ph), 7.64 (s, 8H, BAr'4). 13C{1H} NMR (−20 °C, CD2Cl2, 75 MHz): δ 16.4 (s, PCHMe2), 16.6 (d, 2JCP = 7 Hz, CH2), 16.9 (d, 2JCP = 5 Hz, PCHMe2), 17.7 (s, MeC(O)N), 23.3 (s, N{(CHMe2)2C6H3}), 23.8 (s, N{(CHMe2)2C6H3}), 28.9 (s, N{(CHMe2)2C6H3}), 29.3 (d, 1JCP = 25 Hz, PCHMe2), 32.5 (s, CMe2), 40.3 (s, CMe2), 117.4 (s, BAr'4), 119.4 (s, o-CHar, Ph), 124.6 (s, m-CHar, N-Ar), 125.0 (q, 1JCF = 272 Hz, CF3 BAr'4), 127.8 (s, p-CHar, N-Ar), 129.3 (q, 2JCF = 31 Hz, BAr'4), 130.1 (s, p-CHar, Ph), 130.3 (s, ipso-Car, Ph), 134.4 (s, m-CHar, Ph), 135.2 (s, BAr'4), 139.1 (s, o-Car, N-Ar), 139.4 (s, ipso-Car, N-Ar), 166.2 (q, 1JCB = 50 Hz, B-Car), 169.7 (s, MeC(O)N). 31P{1H} NMR (25 °C, CD2Cl2, 121 MHz): δ 185.7 (s).

Synthesis of complex 7a. Method A: 261 mg (0.5 mmol) of compound 5 was dissolved in 20 mL of acetonitrile at −40 °C. The mixture was allowed to reach room temperature over 30 min. Solvent was then evaporated under vacuum, and the orange residue was rinsed with 20 mL of hexane and recrystallized from Et2O:hexane (2:1) at −10 °C. Yield: 63% (0.45 g). Method B: A solution of 1.08 g (1.07 mmol) of H(Et2O)2BAr'4 in 30 mL of acetonitrile was added dropwise to a solution containing 564 mg (1.07 mmol) of compound 3a/a' in 30 mL of acetonitrile at −60 °C. The cooling bath was removed and the reaction mixture was stirred for 30 min. Removal of the solvent under vacuum afforded an orange solid that was rinsed with 2 × 30 mL of hexane and recrystallized from a mixture Et2O:hexane (2:1) at −10 °C to give 7a as an orange crystalline solid. Yield: 69% (1.06 g). Anal. Calcd for C64H62BF24N2NiOP: C, 53.69; H, 4.37; N, 1.96. Found: C, 53.58; H, 4.16; N, 1.88. IR (Nujol mull): ν(C═N) 1617 cm−1, ν(C≡≡N) 2322 cm−1. ESI-MS from MeCN: m/z 526.1 (M+ − CH3CN). CID fragmentation of ion m/z 526.1: m/z 470.1 (M+ − CH3CN − CH2CMe2), 392.0 (M+ − CH3CN − CH2CMe2Ph). 1H NMR (25 °C, CD2Cl2, 300 MHz): δ 0.94 (bs, 3H, NCCH3), 1.13 (d, 6H, 3JHH = 7 Hz, N{(CHMe2)2C6H3}), 1.23 (d, 2H, 3JHP = 11 Hz, CH2), 1.28 (d, 6H, 3JHH = 7 Hz, N{(CHMe2)2C6H3}), 1.42 (s, 6H, CMe2), 1.48 (dd, 6H, 3JHH = 7 Hz, 3JHP = 11 Hz, PCHMe2), 1.55 (dd, 6H, 3JHH = 7 Hz, 3JHP = 13 Hz, PCHMe2), 1.89 (s, 3H, MeC(O)N), 2.47 (m, 2H, PCHMe2), 2.89 (h, 2H, 3JHH = 7 Hz, N{(CHMe2)2C6H3}), 7.06 (t, 1H, 3JHH = 7 Hz, p-CHar, Ph), 7.13–7.20 (m, 3H, m, p-CHar, N-Ar), 7.25 (t, 2H, 3JHH = 8 Hz, m-CHar, Ph), 7.38 (d, 2H, 3JHH = 9 Hz, o-CHar, Ph), 7.48 (s, 4H, BAr'4), 7.64 (s, 8H, BAr'4). 13C{1H}

NMR (CD2Cl2, 75 MHz): δ 1.3 (bs, NCCH3), 16.4 (s, PCHMe2), 17.1 (d, 3JCP = 2 Hz, MeC(O)N), 17.6 (s, PCHMe2), 17.8 (d, 2JCP = 28 Hz, CH2), 23.4 (s, N{(CHMe2)2C6H3}), 27.8 (d, 1JCP = 24 Hz, PCHMe2), 29.1 (s, N{(CHMe2)2C6H3}), 34.2 (s, CMe2), 40.6 (s, CMe2), 117.4 (s, BAr'4), 124.3 (s, p-CHar, Ph), 124.5 (s, m-CHar, N-Ar), 125.0 (q, 1JCF = 272 Hz, CF3), 126.1 (s, o-CHar, Ph), 128.4 (s, p-CHar, N-Ar), 128.4 (s, m-CHar, Ph), 129.3 (q, 2JCF = 31 Hz, CF3-Car), 135.2 (s, BAr'4), 138.4 (s, ipso-Car, N-Ar), 140.6 (s, o-Car, Ph), 151.9 (s, ipso-Car, Ph), 166.2 (q, 1JCB = 50 Hz, B-Car), 171.8 (s, MeC(O)N). 31P{1H} NMR (25 °C, CD2Cl2, 121 MHz): δ 188.7 (s).

Synthesis of complex 7b. Method A: 96 mg (0.06 mmol) of compound 6 was dissolved in 6 mL of acetonitrile. The mixture was stirred for 30 min. Solvent was evaporated under vacuum, and the residue was rinsed with 2 × 5 mL of hexane, extracted with diethyl ether and filtered. The filtrate was evaporated to dryness, leaving the product in quantitative yield. Method B: A solution of 451 mg (0.45 mmol) of H(Et2O)2BAr'4 in 5 mL of acetonitrile was added dropwise to a solution containing 244 mg (0.45 mmol) of compound 3b/b' in 10 mL of acetonitrile at −60 °C. The cooling bath was removed and the reaction mixture was stirred for 2 h. Removal of the solvent under vacuum afforded a white solid that was rinsed with 2 × 10 mL of hexane and recrystallized from a mixture Et2O:hexane (2:1) at −10 °C to give 7b as a colorless crystalline solid. Yield: 72% (0.48 g). Anal. Calcd for C64H62BF24N2OPPd: C, 51.96; H, 4.22; N, 1.89. Found: C, 51.99; H, 4.05; N, 1.81. IR (Nujol mull): ν(C═N) 1635 cm−1, ν(C≡≡N) 2322 cm−1. ESI-MS from MeCN: m/z 574.1 (M+ − CH3CN). CID fragmentation of ion m/z 574.1: m/z 518.1 (M+ − CH3CN − CH2CMe2), 442.0 (M+ − CH3CN − CH2CMe2Ph). 1H NMR (25 °C, CD2Cl2, 300 MHz): δ 1.12 (d, 6H, 3JHH = 7 Hz, N{(CHMe2)2C6H3}), 1.22 (d, 6H, 3JHH = 7 Hz, N{(CHMe2)2C6H3}), 1.31 (dd, 6H, 3JHH = 7 Hz, 3JHP = 2 Hz, PCHMe2), 1.32 (bs, 3H, NCCH3), 1.36 (d, 6H, 3JHH = 7 Hz, PCHMe2), 1.41 (s, 6H, CMe2), 1.93 (s, 3H, MeC(O)N), 2.05 (d, 2H, 3JHP = 5 Hz, CH2), 2.26 (m, 2H, PCHMe2), 2.70 (h, 2H, 3JHH = 7 Hz, N{(CHMe2)2C6H3}), 7.04 (t, 1H, 3JHH = 7 Hz, p-CHar, Ph), 7.16–7.22 (m, 3H, m, p-CHar, N-Ar), 7.28 (t, 2H, 3JHH = 8 Hz, m-CHar, Ph), 7.41 (d, 2H, 3JHH = 7 Hz, o-CHar, Ph), 7.48 (s, 4H, BAr'4), 7.64 (s, 8H, BAr'4). 13C{1H} NMR (25 °C, CD2Cl2, 75 MHz): δ 1.4 (s, NCCH3), 16.4 (s, PCHMe2), 16.7 (d, 3JCP = 2 Hz, MeC(O)N), 17.2 (d, 2JCP = 4 Hz, PCHMe2), 23.3 (s, N{(CHMe2)2C6H3}), 27.5 (bs, CH2), 28.9 (s, N{(CHMe2)2C6H3}), 29.1 (d, 1JCP = 25 Hz, PCHMe2), 33.3 (s, CMe2), 41.0 (s, CMe2), 117.4 (s, BAr'4), 119.8 (s, NCCH3), 124.5 (s, m-CHar, N-Ar), 125.0 (q, 1JCF = 272 Hz, CF3), 125.4 (bs, o-CHar, Ph), 126.7 (s, p-CHar, Ph), 128.0 (s, p-CHar, N-Ar), 129.0 (bs, m-CHar, Ph), 129.3 (q, 2JCF = 31 Hz, CF3-Car), 135.2 (s, BAr'4: o-CHar), 138.6 (s, ipso-Car, N-Ar), 140.2 (s, o-Car, N-Ar), 166.2 (q, 1JCB = 50 Hz, B-Car), 169.3 (s, MeC(O)N). 31P{1H} NMR (25 °C, CD2Cl2, 121 MHz): δ 190.2 (bs).

Synthesis of complex 8a. CO was bubbled through a solution of 478 mg (0.33 mmol) of compound 7a in 10 mL of dichloromethane for 5 min. Solvent was removed under reduced pressure and the resulting residue was rinsed with 10 mL of hexane to afford 8a as a yellow solid. Yield: 89% (0.43 g). IR (Nujol mull): ν(C═N)) 1625 cm−1, ν(C≡≡N) 2321 cm−1. ESI-MS from MeCN: m/z 554.1 (M+ − CH3CN), 526.1 (M+ − CH3CN − CO). CID fragmentation of ion m/z 554.1: m/z 526.1 (M+ − CH3CN − CO), 470.0 (M+ − CH3CN − CO − CH2CMe2), 392.0 (M+ − CH3CN − CO − CH2CMe2Ph); CID fragmentation of ion 526.1: 470.0 (M+ − CH3CN − CO − CH2CMe2), 392.0 (M+ − CH3CN − CO − CH2CMe2Ph). 1H NMR (25 °C, CD2Cl2, 300 MHz): δ 1.18 (s, 3H, NCCH3), 1.18 (d, 6H, 3JHH = 7 Hz, N{(CHMe2)2C6H3}), 1.30 (s, 6H, CMe2), 1.32 (dd, 6H, 3JHH = 8 Hz, 3JHP = 19 Hz, PCHMe2), 1.41 (d, 6H, 3JHH = 7 Hz, N{(CHMe2)2C6H3}), 1.42 (m, 6H, PCHMe2), 1.91 (s, 3H, MeC(O)N), 2.26 (bm, 2H, PCHMe2), 2.89 (h, 2H, 3JHH = 7 Hz,

N{(CHMe2)2C6H3}), 3.32 (s, 2H, CH2), 7.10–7.30 (m, 5H, Ph), 7.10–7.20 (m, 3H, m, p-CHar, N-Ar), 7.48 (s, 4H, BAr'4), 7.64 (s, 8H, BAr'4). 13C{1H} NMR (CD2Cl2, 75 MHz): δ 15.9 (s, PCHMe2), 16.8 (s, PCHMe2), 17.1 (s, MeC(O)N), 23.3 (s, N{(CHMe2)2C6H3}), 23.6 (s, N{(CHMe2)2C6H3}), 27.8 (d, 1JCP = 23 Hz, PCHMe2), 28.8 (s, N{(CHMe2)2C6H3}), 29.2 (s, CMe2), 38.5 (s, CMe2), 68.1 (d, 3JCP = 6 Hz, CH2), 117.4 (s, BAr'4), 124.5 (s, m-CHar, N-Ar), 125.0 (q, 1JCF = 272 Hz, CF3), 125.7 (s, o-CHar, Ph), 126.3 (s, p-CHar, Ph), 128.3 (s, p-CHar, N-Ar'), 128.4 (s, m-CHar, Ph), 129.3 (q, 2JCF = 31 Hz, CF3-Car), 135.2 (s, BAr'4: o-CHar), 138.1 (s, ipso-Car, N-Ar), 140.3 (s, o-Car, N-Ar), 147.8 (s, ipso-Car, Ph), 166.2 (q, 1JCB = 50 Hz, B-Car), 171.8 (s, MeC(O)N), 241.5 (d, 2JCP = 10 Hz, CO). 31P{1H} NMR (25 °C, CD2Cl2, 121 MHz): δ 181.4 (s).

Synthesis of complex 8b. A Fischer Porter reactor was flushed with nitrogen and 295 mg (0.2 mmol) of compound 7b was transferred in 10 mL of dichloromethane. The reactor was charged with CO at 4 bar, and the reaction mixture was stirred at room temperature for 1 h. The solution was taken to dryness and the resulting yellow solid was recrystallized from a mixture Et2O:hexane (2:1) at −10 °C to give 8b as a colorless crystalline solid. Yield: 56% (0.17 g). IR (Nujol mull): ν(C═N) 1638 cm−1, ν(C≡≡N) 2320 cm−1, ν(CO) 1728 cm−1. Anal. Calcd for C65H62BF24N2O2PPd: C, 51.79; H, 4.15; N, 1.86. Found: C, 51.75; H, 4.24; N, 1.88. ESI-MS from MeCN: m/z 574.2 (M+ (CH3CN − CO); CID fragmentation of ion m/z 574.2: m/z 518.0 (M+ − CH3CN − CO − CH2CMe2), 440.0 (M+ − CH3CN − CO − CH2CMe2Ph). 1H NMR (25 °C, CD2Cl2, 300 MHz): δ 1.17 (d, 6H, 3JHH = 7 Hz, N{(CHMe2)2C6H3}), 1.24 (dd, 6H, 3JHH = 7 Hz, 3JHP = 4 Hz, PCHMe2), 1.31 (d, 6H, 3JHH = 7 Hz, N{(CHMe2)2C6H3}), 1.34 (dd, 6H, 3JHH = 7 Hz, 3JHP = 4 Hz, PCHMe2), 1.36 (s, 6H, CMe2), 1.59 (s, 3H, NCCH3), 1.96 (s, 3H, MeC(O)N), 2.25 (m, 2H, PCHMe2), 2.75 (h, 2H, 3JHH = 7 Hz, N{(CHMe2)2C6H3}), 3.12 (s, 2H, CH2), 7.04–7.30 (m, 5H, Ph), 7.15–7.30 (m, 3H, m, p-CHar, N-Ar), 7.48 (s, 4H, BAr'4), 7.64 (s, 8H, BAr'4). 13C{1H} NMR (25 °C, CD2Cl2, 75 MHz): δ 1.5 (s, NCCH3), 16.1 (s, PCHMe2), 16.6 (d, 2JCP = 6 Hz, PCHMe2), 16.8 (s, MeC(O)N), 23.3 (s, N{(CHMe2)2C6H3}), 23.7 (s, N{(CHMe2)2C6H3}), 28.2 (d, 1JCP = 22 Hz, PCHMe2), 28.8 (s, N{(CHMe2)2C6H3}), 29.0 (s, CMe2), 38.9 (s, CMe2), 69.7 (d, 3JCP = 21 Hz, CH2), 117.4 (s, BAr'4), 124.5 (s, m-CHar, N-Ar), 125.0 (q, 1JCF = 272 Hz, CF3), 125.8 (s, o-CHar, Ph), 126.4 (s, p-CHar, N-Ar), 128.0 (s, p-CHar, N-Ar), 128.5 (s, m-CHar, Ph), 129.3 (q, 2JCF = 31 Hz, CF3-Car), 135.2 (s, BAr'4), 138.3 (s, ipso-Car, o-C6H4), 140.0 (s, o-Car, N-Ar), 147.8 (s, ipso-Car, Ph), 166.2 (q, 1JCB = 50 Hz, B-Car), 169.5 (s, MeC(O)N), 219.9 (d, 2JCP = 10 Hz, CO). 31P{1H} NMR (25 °C, CD2Cl2, 121 MHz): δ 176.3 (s).

Synthesis of compound 9. A Fischer Porter reactor was flushed with nitrogen and charged with 20 mL of toluene and a mixture of ethylene:CO 1:1 at 6 bar. After stabilizing the temperature at 60 °C, a solution of 200 mg (0.14 mmol) of compound 6 in 2 mL of dichloromethane was transferred with a syringe counter pressure through a septum-capped port. The reaction mixture was stirred for 1 h. The solution was then filtered to remove Pd(0) traces, and the solvent was removed under vacuum. The resulting solid was rinsed with 5 mL of hexane and recrystallized from a mixture Et2O:hexane (2:1) at −10 °C. Compound 9 was obtained as a colorless crystalline solid in 62% yield (277 mg). IR (Nujol mull): ν(C═N) 1609 cm−1, ν(C═O) 1734 cm−1. Anal. Calcd for C65H63BF24N2O2PPd: C, 52.24; H, 4.25; N, 0.94. Found: C, 52.58; H, 4.48; N, 1.13. ESI-MS from toluene: m/z 630.1 (M+). CID fragmentation of ion m/z 630.1: m/z 573.1 (M+ − C2H4 − CO), 517.0 (M+ − C2H4 − CO − CH2CMe2), 440.0 (M+ − C2H4 − CO − CH2CMe2Ph). 1H NMR (25 °C, CD2Cl2, 300 MHz): δ 1.09 (s, 6H, CH2CMe2-o-C6H4), 1.14 (d, 6H, 3JHH = 7 Hz, N{(CHMe2)2C6H3}), 1.19 (d, 6H, 3JHH = 7 Hz, N{(CHMe2)2C6H3}), 1.28 (dd, 6H,

3JHH = 7 Hz, 3JHP = 20 Hz, PCHMe2), 1.37 (dd, 6H, 3JHH = 7 Hz, 3JHP = 17 Hz, PCHMe2), 1.56 (td, 2H, 3JHH = 6 Hz, 3JHP = 2 Hz, PdCH2CH2CO), 1.99 (s, 3H, MeC(O)N), 2.41 (m, 2H, PCHMe2), 2.67 (t, 2H, 3JHH = 6 Hz, PdCH2CH2CO), 2.82 (h, 2H, 3JHH = 7 Hz, N{(CHMe2)2C6H3}), 2.86 (s, 2H, CH2CMe2), 7.11 (d, 1H, 3JHH = 7 Hz, o-CHar, Ph), 7.19 (t, 2H, 3JHH = 7 Hz, m-CHar, Ph), 7.22–7.29 (m, 3H, o, m-CHar, N-Ar), 7.33 (dd, 2H, 3JHH = 9 Hz, 3JHH = 7 Hz, p-CHar, Ph), 7.48 (s, 4H, BAr'4), 7.64 (s, 8H, BAr'4). 13C{1H} NMR (25 °C, CD2Cl2, 75 MHz): δ 12.4 (s, PdCH2CH2CO), 16.0 (d, 3JCP = 3 Hz, MeC(O)N), 16.4 (s, PCHMe2), 16.7 (d, 2JCP = 5 Hz, PCHMe2), 22.9 (s, N{(CHMe2)2C6H3}), 23.9 (s, N{(CHMe2)2C6H3}), 28.8 (s, CMe2), 29.0 (s, N{(CHMe2)2C6H3}), 29.4 (d, 1JCP = 27 Hz, PCHMe2), 37.9 (s, CMe2), 52.3 (s, PdCH2CH2CO), 53.7 (s, CH2CMe2), 117.4 (s, BAr'4: pCHar), 124.5 (s, m-CHar, N-Ar), 125.0 (q, 1JCF = 272 Hz, CF3), 125.3 (s, o-CHar, Ph), 126.8 (s, p-CHar, Ph), 128.6 (s, p-CHar, N-Ar), 128.9 (s, m-CHar, Ph), 129.3 (q, 2JCF = 31 Hz, CF3-Car), 135.2 (s, BAr'4), 138.5 (s, ipso-Car, N-Ar), 140.0 (s, o-Car, N-Ar), 147.0 (s, ipso-Car, Ph), 166.2 (q, 1JCB = 50 Hz, B-Car), 169.4 (s, MeC(O)N), 235.6 (s, PdCH2CH2CO). 31P{1H} NMR (25 °C, CD2Cl2, 121 MHz): δ 194.6 (s).

Reaction of complex 6 with CO. **Observation of compounds 10 and 11.** A thick-walled NMR tube fitted with a Young PTFE valve was charged with a CD2Cl2 solution of compound 6 and CO at 4 bar. 31P{1H} spectra were recorded at different temperatures between 30 °C and −20 °C. Two signals were observed, corresponding to compounds 10 and 11. The position of the signals varied only slightly with the temperature but their intensity ratio changed significantly: 1:1 at 30 °C; 1:3 at 25 °C, and 1:6 at −20 °C. Resonances of the minor product 10 were partially obscured by those of 11. Compound 10: 1H NMR (−20 °C, CD2Cl2, 500 MHz): δ 1.02 (bd, 6H, N{(CHMe2)2C6H3}), 1.94 (bs, 3H, MeC(O)N), 2.58 (bm, 2H, N{(CHMe2)2C6H3}), 7.39 (bd, 1H, o-CHar, Ph). 13C{1H} NMR (−20 °C, CD2Cl2, 125 MHz): 16.3 (s, PCHMe2), 16.8 (d, 2JCP = 4.5 Hz, PCHMe2) 23.4 (s, N{(CHMe2)2C6H3}), 23.5 (s, N{(CHMe2)2C6H3}), 28.9 (d, 1JCP = 31 Hz, PCHMe2), 32.8 (bs, CMe2), 36.3 (bs, CMe2), 140.2 (s, o-Car, N-Ar). 31P{1H} (−20 °C, CD2Cl2, 202 MHz): δ 186.3 (bs). Compound 11: 1H NMR (−20 °C, CD2Cl2, 500 MHz): δ 1.14 (d, 6H, 3JHH = 7 Hz, N{(CHMe2)2C6H3}), 1.18 (dd, 6H, 3JHH = 7 Hz, 3JHP = 11 Hz, PCHMe2), 1.30 (d, 6H, 3JHH = 7 Hz, N{(CHMe2)2C6H3}), 1.31 (dd, 6H, 3JHH = 7 Hz, 3JHP = 14 Hz, PCHMe2), 1.38 (s, 6H, CMe2), 1.99 (s, 3H, MeC(O)N), 2.23 (m, 2H, PCHMe2), 2.71 (h, 2H, 3JHH = 7 Hz, N{(CHMe2)2C6H3}), 3.16 (s, 2H, CH2), 7.17 (t, 1H, 3JHH = 7.2 Hz, p-CHar, Ph), 7.20–7.23 (m, 3H, m, p-CHar, N-Ar), 7.26 (d, 2H, 3JHH = 8.6 Hz, o-CHar, Ph), 7.30 (t, 2H, 3JHH = 7.2 Hz, m-CHar, Ph), 7.48 (s, 4H, BAr'4), 7.64 (s, 8H, BAr'4). 13C{1H} NMR (CD2Cl2, −20 °C): δ 15.9 (s, MeC(O)N), 16.4 (s, PCHMe2), 16.5 (d, 2JCP = 5.8 Hz, PCHMe2), 23.3 (s, N{(CHMe2)2C6H3}), 23.7 (s, N{(CHMe2)2C6H3}), 28.2 (d, 1JCP = 20 Hz, PCHMe2), 29.0 (s, N{(CHMe2)2C6H3}), 29.6 (s, CMe2), 39.2 (s, CMe2), 73.2 (d, 3JCP = 20 Hz, CH2), 117.4 (s, BAr'4), 124.7 (s, m-CHar, N-Ar), 125.0 (q, 1JCF = 272 Hz, CF3), 125.8 (s, o-CHar, N-Ar), 127.1 (s, p-CHar, Ph), 128.8 (s, p-CHar, N-Ar), 128.9 (s, m-CHar, Ph), 129.3 (q, 2JCF = 31 Hz, CF3-Car), 135.2 (s, BAr'4), 138.5 (s, ipso-Car, N-Ar), 138.9 (s, o-Car, N-Ar), 146.7 (s, ipso-Car, Ph), 166.2 (q, 1JCB = 50 Hz, B-Car), 171.7 (s, MeC(O)N), 215.6 (s, CO). 31P{1H} NMR (−20 °C, CD2Cl2, 202 MHz): δ 169.9 (s). Solution IR (CH2Cl2, CO, 4 bar, 293 K): 1712 cm−1 (ν(*C*═O) acyl; coordinate CO bands were not observed, due to overlapping with the free *C*═O absorption).

Reaction of compound 6 with 13CO. 13CO was bubbled through a CD2Cl2 solution of 6, cooled to −60 °C. 13C{1H} NMR (−60 °C, CD2Cl2, 100 MHz), selected data: δ 172.6 (d, 2JCP = 79.4 Hz,

Pd-CO, 10); 175.6 (d, 2JCP = 117 Hz, Pd-CO, 11); 216.4 (s, Pd-C(O)-R, 11). 31P{1H} NMR (−60 °C, CD2Cl2, 161 MHz): δ 169.9 (d, 2JPC = 79.4 Hz, 11); 185.7 (s, 6); 186.6 (d, 2JPC = 115 Hz, 10).

X-ray structure analysis for 3b, 3b', 4, 6, 7a, 7b, 8b and 9. A summary of crystallographic data and structure refinement results for these new crystalline compounds is given in Table 1. Crystals coated with dry perfluoropolyether were mounted on glass fibers and fixed in a cold nitrogen stream. Intensity data were collected on a Bruker-Nonius X8Kappa Apex II CCD diffractometer (3b/3b', 4, 7a, 7b, 8b and 9) equipped with a graphite monochromator to obtain λ(Mo Kα) = 0.71073 Å radiation, or on a Bruker SMART 6000 CCD area-detector diffractometer (6) equipped with a laboratory rotating anode source, coupled to Göbel mirror optics to obtain a monochromated Cu-Kα (λ = 1.54184 Å) radiation. The data were reduced by SAINT86 and corrected for absorption effects by the multi-scan method (SADBAS).87 The structures were solved by direct methods (SIR-2002)88 and refined against all F2 data by full-matrix least squares techniques (SHELXTL-6.12)89 minimizing w[Fo2 − Fc2]2. All non-hydrogen atoms were refined with anisotropic thermal parameters. Hydrogen atoms were included in calculated positions and refined allowing to ride on their respective attached carbon atoms with the isotropic temperature factors (Uiso values) fixed at 1.2 times (1.5 times for the methyl group) the Ueq values of the corresponding carbon atoms.

Acknowledgements

Financial support from the DGI (Project CTQ2009-11721), Junta de Andalucía (Project P09-FQM5074) and EU (FEDER Funds) is gratefully acknowledged. I.M. thanks a postdoctoral contract from the Junta de Andalucía.

References

1.Olefin Upgrading Catalysis by Metal Complexes, State-of-the Art and Perspectives, ed. G. Giambastiani and J. Cámpora, Springer, Dordrecht, 2011

2.A. Nakamura, S. Ito and K. Nozaki, Chem. Rev., 2009, 109, 5215–5244

3.Metal Catalysts in Olefin Polymerization, ed. Z. Guan, Springer-Verlag, Berlin, 2009

4.Late Transition Metal Polymerization Catalysis, ed. B. Rieger, L. S. Baugh, S. Kacker and S. Striegler, Wiley, Weinheim, 2003

5.V. C. Gibson and S. K. Sptizmesser, Chem. Rev., 2003, 103, 283

6.C. Bianchini and A. Meli, Coord. Chem. Rev., 2002, 225, 35

7.S. D. Ittel and L. K. Johnson, Chem. Rev., 2000, 100, 1169

8.E. Drent and P. H. M. Budzelaar, Chem. Rev., 1996, 96, 663

9.A. Ravasio, L. Boggini and I. Tritto, in Olefin Upgrading Catalysis by Nitrogen-Based Metal Complexes, ed. G. Giambastiani and J. Cámpora, Springer, Dorderecht, 2011, vol. 1, pp. 27–118

10.D. H. Camacho and Z. Guan, Chem. Commun., 2010, 46, 7879

11.P. Braunstein, Chem. Rev., 2006, 106, 134

12.F. Speiser, P. Braunstein and L. Sausine, Acc. Chem. Res., 2005, 38, 784

13.P. Braunstein and F. Naud, Angew. Chem., Int. Ed., 2001, 40, 680

14.W. Keim, Angew. Chem., Int. Ed. Engl., 1990, 29, 235

15.F. Hasanayn, P. Achord, P. Braunstein, H. J. Magnier, K. Krogh-Jaspersen and A. S. Goldman, Organometallics, 2012, 31, 4680

16.P. Braunstein, Y. Chauvin, S. Mercier and L. Saussine, C. R. Chim., 2005, 8, 31

17.E. F. Connor, T. R. Younkin, J. I. Henderson, S. Hwang, R. H. Grubbs, W. P. Roberts and J. L. Litzau, J. Polym. Sci., Part A: Polym. Chem., 2002, 40, 2842

18.T. R. Younkin, E. F. Connor, J. I. Henderson, S. K. Friedrich and R. H. Grubbs, Science, 2000, 287, 460

19.C. M. Wang, S. Friedrich, T. R. Younkin, R. T. Li, R. H. Grubbs, D. A. Bansleben and M. W. Day, Organometallics, 1998, 17, 3149

20.B. Korthals, I. Götter-Schnetmann and S. Mecking, Organometallics, 2007, 26, 1311

21.W. Keim, S. Killar, C. F. Nobile, G. P. Suranna, U. Englert, R. Wang, S. Mecking and D. L. Schröder, J. Organomet. Chem., 2002, 662, 150

22.Z. Guan and W. J. Marshall, Organometallics, 2002, 21, 3580

23.O. Daugulis and M. Brookhart, Organometallics, 2002, 21, 5928

24.M. C. Bonnet, F. Dahan, A. Ecke, W. Keim, R. P. Schulz and I. Tatchenko, J. Chem. Soc., Chem. Commun., 1994, 615

25.H.-P. Chen, Y.-H. Liu, S.-M. Peng and S.-T. Liu, Organometallics, 2003, 22, 4893

26.H. Y. Kwon, S. Y. Lee, S. M. Shin and Y. K. Chung, Dalton Trans., 2004, 921

27.F. Speiser, P. Braunstein, L. Saussine and R. Welter, Inorg. Chem., 2004, 43, 1649

28.F. Speiser, P. Braunstein and L. Saussine, Organometallics, 2004, 23, 2625

29.F. Speiser, P. Braunstein and L. Saussine, Organometallics, 2004, 23, 2633

30.F. Speiser, P. Braunstein, L. Saussine and R. Walter, Organometallics, 2004, 23, 2613

31.A. Kermagoret and P. Braunstein, Organometallics, 2008, 27, 88

32.J. Flapper, H. Kooijman, M. Lutz, A. L. Spek, P. W. N. M. van Leeuwen, C. J. Elsevier and P. C. J. Kamer, Organometallics, 2009, 28, 3272

33.J. Flapper, P. W. N. M. van Leeuwen, C. J. Elsevier and P. C. J. Kamer, Organometallics, 2009, 28

34.M. M. Mogorosi, T. Mahamo, J. R. Moss, S. F. Mapolie, J. C. Slootweg, K. Lammertsma and G. S. Smith, J. Organomet. Chem., 2011, 696, 3585

35.P. Braunstein, J. Pietsch, Y. Chauvin, S. Mercier, L. Saussine, A. DeCian and J. Fischer, J. Chem. Soc., Dalton Trans., 1996, 3571

36.K. S. Coleman, M. L. H. Green, S. I. Pascu, N. H. Rees, A. R. Cowley and L. H. Rees, J. Chem. Soc., Dalton Trans., 2001, 3384

37.P. Y. Lee and L. C. Liang, Inorg. Chem., 2008, 47, 749

38.S. Mecking, Coord. Chem. Rev., 2000, 203, 325

39.T. M. J. Anselment, S. I. Vagin and B. Rieger, Dalton Trans., 2008, 4537

40.E. K. van den Beuken, W. J. J. Smeets, A. L. Spek and B. L. Feringa, Chem. Commun., 1998, 223

41.O. Daugulis, M. Brookhart and P. S. White, Organometallics, 2002, 21, 5935

42.H. R. Wu, Y. H. Liu, S. M. Peng and S. T. Liu, Eur. J. Inorg. Chem., 2004, 3152

43.K. R. Reddy, C. L. Chen, S. M. Peng, J. T. Chen and S. T. Liu, Organometallics, 1999, 18, 2574

44.K. R. Reddy, W. W. Tsai, K. Surekha, G. H. Lee, S. M. Peng, J. T. Chen and S. T. Liu, J. Chem. Soc., Dalton Trans., 2002, 1776

45.A. D. Burrows, M. F. Mahon and M. Varrone, Dalton Trans., 2003, 4718

46.K. R. Reddy, K. Surekha, G. H. Lee, S. M. Peng, J. T. Chen and S. T. Liu, Organometallics, 2001, 20, 1292

47.M. Agostinho and P. Braunstein, Chem. Commun., 2007, 58

48.M. Agostinho, P. Braunstein and R. Welter, Dalton Trans., 2007, 759

49.P. Braunstein, J. Pietsch, Y. Chauvin, A. DeCian and J. Fischer, J. Organomet. Chem., 1997, 529, 387

50.P. Braunstein, J. Pietsch, Y. Chauvin, A. DeCian and J. Fischer, J. Organomet. Chem., 1999, 582, 371

51.M. J. Rachita, R. L. Huff, J. L. Bennett and M. Brookhart, J. Polym. Sci., Part A: Polym. Chem., 2000, 38, 4627

52.J. Pietsch, P. Braunstein and Y. Chauvin, New J. Chem., 1998, 22, 467

53.H. Y. Wang and G. X. Jin, Eur. J. Inorg. Chem., 2005, 1665

54.L. Ortiz de la Tabla, I. Matas, P. Palma, E. Álvarez and J. Cámpora, Organometallics, 2012, 31, 1006

55.J. Cámpora, M. M. Conejo, K. Mereiter, P. Palma, C. Pérez, M. L. Reyes and C. Ruiz, J. Organomet. Chem., 2003, 683, 220

56.J. Cámpora, J. A. López, P. Palma, D. del Río, E. Carmona, P. Valerga, C. Graiff and A. Tiripicchio, Inorg. Chem., 2001, 40, 4116

57.N. G. Jones, M. L. H. Green, I. Vei, A. Cowley, X. Morise and P. Braunstein, J. Chem. Soc., Dalton Trans., 2004, 1487

58.J. N. Harvey, K. M. Heslop, A. G. Orpen and P. G. Pringle, Chem. Commun., 2003, 278

59.O. del Campo, A. Carbayo, J. V. Cuevas, G. García-Herbosa and A. Muñoz, Eur. J. Inorg. Chem., 2009, 2254

60.E. Carmona, E. Gutiérrez-Puebla, J. M. Marín, A. Monge, M. Paneque, M. L. Poveda and C. Ruíz, J. Am. Chem. Soc., 1989, 111, 2883

61.J. Cámpora, J. A. López, P. Palma, P. Valerga, E. Spillner and E. Carmona, Angew. Chem., Int. Ed., 1999, 38, 147

62.J. Cámpora, E. Gutiérrez-Puebla, J. A. López, A. Monge, P. Palma, D. del Río and E. Carmona, Angew. Chem., Int. Ed., 2001, 40, 3641

63.G. A. Olah and C. W. McFarland, J. Org. Chem., 1969, 34, 1832

64.The spectra of the phosphonium salt look unexpectedly clear because the signals for the 2,6-diisopropylphenyl fragment disappear from the spectrum once decomposition of 5 has

taken place. We have no indications of what could be the final fate of the imine fragment, but it is possible that these could be forming part of a paramagnetic species.

65.K. R. Reddy, K. Surekha, G. H. Lee and S. M. Peng, Organometallics, 2001, 20, 5557

66.M. Catellani, C. Mealli, P. Motti, P. Paoli, E. Pérez-Carreño and P. S. Pregosin, J. Am. Chem. Soc., 2002, 124, 4336

67.J. W. Faller and N. Sarantopoulos, Organometallics, 2004, 23, 2008

68.U. Christmann, D. Patanzis, J. Benet-Bucholz, J. E. McGrady and R. Vilar, J. Am. Chem. Soc., 2006, 128, 6376

69.D. I. Chai, P. Thansandote and M. Lautens, Chem.–Eur. J., 2011, 17, 8175

70.K. D. Klatchavili, D. J. Mindiola and G. L. Hillhouse, J. Am. Chem. Soc., 2004, 126, 10554

71.R. A. Michelin, M. Mozzon and R. Bertani, Coord. Chem. Rev., 1996, 147, 299

72.B. M. Markies, D. Kruis, M. H. P. Rietveld, K. A. N. Verkerk, J. Boersma, H. Kooijman, M. T. Lakin, A. L. Spek and G. van Koten, J. Am. Chem. Soc., 1995, 117, 5263

73.R. Luo, D. K. Newsham and A. Sen, Organometallics, 2009, 21, 5382

74.I. Liu, B. T. Heaton, J. A. Iggo, R. Whytman, J. F. Bickley and A. Steiner, Chem.–Eur. J., 2006, 12, 4417

75.M. Gómez, S. Jensat, G. Muller, D. Panyella, P. W. N. M. van Leeuwen, P. C. J. Kamer, K. Goubitz and J. Fraanje, Organometallics, 1999, 18, 4970

76.G. C. P. M. Dekker, A. Buijs, C. J. Elsevier, K. Vrieze, P. W. N. M. van Leeuwen, W. J. J. Smeets, A. L. Spek, Y. F. Wang and C. H. Stam, Organometallics, 1992, 11, 1937

77.C. S. Schultz, J. Ledford, J. DeSimone and M. Brookhart, J. Am. Chem. Soc., 2000, 122, 6531 .

78.F. C. Rix, M. Brookhart and P. S. White, J. Am. Chem. Soc., 1996, 118, 4746

79.R. van Asselt, E. E. C. G. Gielens, R. E. Rulke, K. Vrieze and C. J. Elsevier, J. Am. Chem. Soc., 1994, 116, 977

80.J. J. Curley, K. D. Kitiachivili, R. Waterman and G. L. Hillhouse, Organometallics, 2009, 28, 2568

81.M. Agostinho and P. Braunstein, C. R. Chim., 2007, 10, 666

82.P. Braunstein, J. Durand, M. Knorr and C. Strohman, Chem. Commun., 2001, 211

83.P. Braunstein, C. Frison and X. Morise, Angew. Chem., Int. Ed., 2000, 39, 2867

84.M. Brookhart, B. Grant and A. F. Volpe, Organometallics, 1992, 11, 3920

85.R. T. Boeré, V. Klassen and G. Wolmershäusser, J. Chem. Soc., Dalton Trans., 1998, 4147

86.Bruker APEX2, Bruker AXS Inc, Madison, Wisconsin, USA, 2007

87.Bruker APEX2, Bruker AXS Inc, Madison, Wisconsin, USA, 2001

88.C. M. Burla, B. Camalli, B. Carrozini, G. L. Cascarano, S. Giacovazzo, G. Poliori and R. Spagna, SIR2002: the program, J. Appl. Crystallogr., 2003, 36, 1103

89.G. M. Sheldrick, Acta Crystallogr., Sect. A: Found. Crystallogr., 2007, 64, 112

Footnotes

† Dedicated to Prof. David J. Cole-Hamilton on the occasion of his retirement and for his outstanding contribution to transition metal catalysis. An outstanding scientist, an excellent supervisor, and a wonderful friend.

‡ CCDC reference numbers 876279–876285 for 3b, 3b', 4, 6, 7a, 7b, 8b and 9. For crystallographic data in CIF or other electronic format see DOI: 10.1039/c2dt31334k

Figure captions

Figure 1. Crystal structure of 3b. Selected bond distances (Å) and angles (°): Pd2–P2, 2.2867(9); Pd2–N2 2.173(2); Pd2–C51, 2.081(3); Pd2–C56, 2.008(3); P2–O2, 1.700(2); C43–O2, 1.358(4); C43–N2, 1.280(4); P2–Pd2–N2, 79.42(7); C51–Pd2–C56, 79.62(14); C51–C52–C55–C(56), 24.0(4); N2–Pd2–P2–O2, 5.91(9).

Figure 2. Crystal structure of 3b'. Selected bond distances (Å) and angles (°): Pd1–P1, 2.2453(8); Pd1–N1 2.215(3); Pd1–C21, 2.049(3); Pd1–C26, 2.076(3); P1–O1, 1.693(2); C13–O1, 1.359(4); C13–N1, 1.283(4); P1–Pd1–N1, 78.95(7); C21–Pd1–C26, 79.59(13); C21–C22–C25–C26, 27.3(4); N1–Pd1–P1–O1, 3.73(11).

Figure 3. Crystal structure of **4**. Selected bond distances (Å) and angles (°): Pd1–P1, 2.2939(3); Pd1–O1 2.1854(9); Pd1–C8, 2.0431(12); Pd1–C1, 2.0241(13); P1–N1, 1.7765(11); C12–N1, 1.3777(17); C12–O1, 1.2366(16); P1–Pd1–O1, 79.27(3); C8–Pd1–C1, 79.00(5); C8–C7–C6–C1, 26.10(14); O1–Pd1–P1–N1, 10.14(5).

Figure 4. ESI-MS spectrum of compound 6. Upper part: full spectrum. The inset shows an expansion of M+, and calculated isotope pattern. Lower part, CID fragmentation of M+.

Figure 5. Crystal structure of 6. Selected bond distances (Å) and angles (°): Pd1–C1, 2.074(4); Pd1—P1, 2.1712(13); Pd1–N1, 2.172(4); Pd1–C(3), 2.491(5); Pd–C(4) 2.463(5); C3–C4, 1.403(7); C3–C8, 1.404(7); C23–N1, 1.280(6); C23–O1, 1.344(6); P1–Pd1–N1, 81.55(11); N1–Pd1–C1, 171.87(15); P1–Pd1–C1, 92.75(14); C1–C2–C3–C4, 46.2(5).

Figure 6. Crystal structure of 7a. Selected bond distances (Å) and angles (°): Ni1–C21, 1.971(3); Ni1–N2, 1.893(3); Ni1–N1, 1.984(2); Ni1–P1, 2.0880(8); C13–N1, 1.282(4); C13–O1, 1.356(4); P1–O1, 1.683(2); C21–Ni1–N2, 95.51(6); P1–Ni1–N1, 83.78(7).

Figure 7. Crystal structure of 7b. Selected bond distances (Å) and angles (°): Pd1–C21, 2.0657(14); Pd1–N2, 2.0881(13); Pd1–N1, 2.1572(12); Pd1–P1, 2.1893(4); C13–N1, 1.2796(19); C13–O1, 1.3510(18); P1–O1, 1.6820(11); C21–Pd1–N2, 88.73(25); P1–Pd1–N1, 81.68.

Figure 8. Crystal structure of 8b. Selected bond distances (Å) and angles: Pd1–C21, 2.006(5); Pd1–N2, 2.089(4); Pd1–N1, 2.167(4); Pd–P1, 2.2097(12); C21–O2, 1.107(7); C13–N1, 1.283(6); C13–O1, 1.360(6); C21–Pd1–N2, 88.21(19); P1–Pd1–N1, 81.38(11); Pd1–C21–O2, 121.2(5); C22–C21–Pd1, 109.8(4).

Figure 9. Crystal structure of 9. Selected bond distances (Å) and angles: Pd1–C21, 2.039(6); Pd1–N1, 2.124(5); Pd–P1, 2.1682(16); Pd1–O2, 2.133(4) C23–O2, 1.237(2); C13–N1, 1.287(8); C13–O1, 1.352(7); C21–Pd1–O2, 81.9(2); P1–Pd1–N1, 81.84(14); C21–C22–C23–O2, 22.8(8).

Table 1

Table 1 Summary of crystallographic data and structure refinement results for **3b**/**3b′**, **4**, **6**, **7a**, **7b**, **8b** and **9**

Compound	**3b/3b′**	**4**	**6**	**7a**	**7b**	**8b**	**9**
Chemical formula	$C_{30}H_{46}NOPPd$	$C_{30}H_{46}NOPPd$	$C_{30}H_{47}NOPPd \cdot C_{32}H_{12}BF_{24}$	$C_{32}H_{50}N_2NiOPd \cdot C_{32}H_{12}BF_{24}$	$C_{32}H_{50}N_2OPPd \cdot C_{32}H_{12}BF_{24}$	$C_{33}H_{50}N_2O_2PPd \cdot C_{32}H_{12}BF_{24}$	$C_{33}H_{51}NO_2PPd \cdot C_{32}H_{12}BF_{24}$
Formula mass	574.05	574.05	1438.28	1431.65	1479.34	1507.35	1494.34
Crystal system	Monoclinic	Monoclinic	Triclinic	Triclinic	Monoclinic	Triclinic	Monoclinic
a/Å	10.3755(12)	15.6645(5)	12.419(3)	12.26610(10)	41.0211(6)	12.3365(9)	17.3921(5)
b/Å	47.445(6)	12.6885(4)	13.523(3)	20.4994(2)	12.5738(2)	13.3092(11)	16.3003(5)
c/Å	12.2103(16)	14.5290(5)	19.347(4)	27.7574(3)	26.4997(4)	21.2562(18)	24.2674(7)
α/°	90.00	90.00	78.15(3)	103.1860(10)	90.00	106.599(4)	90.00
β/°	90.737(5)	92.6740(10)	82.33(3)	92.1610(9)	97.5640(10)	96.181(4)	107.0410(10)
γ/°	90.00	90.00	82.15(3)	102.9160(10)	90.00	92.774(4)	90.00
Unit cell	6010	2884.6	3131.5(11)	6594.59(11	13549.4(4)	3313.7(5)	6577.7(3)

Compound	**3b/3b'**	**4**	**6**	**7a**	**7b**	**8b**	**9**
volume/Å^3	.2(13)	3(16)		)			
Temperature/K	100(2)	100(2)	120(2)	100(2)	100(2)	100(2)	100(2)
Space group	$P2_1/c$	$P2_1/c$	$P\bar{1}$	$P\bar{1}$	$C2/c$	$P\bar{1}$	$P2_1/n$
No. of formula units per unit cell, Z	8	4	2	4	8	2	4
Radiation type	MoKα	MoKα	CuKα	MoKα	MoKα	MoKα	MoKα
Absorption coefficient, μ/mm^{-1}	0.692	0.720	3.651	0.429	0.405	0.417	0.419
No. of reflections measured	37 027	28 673	10 135	57 638	53 449	11 840	61 756
No. of independent reflections	10 798	7280	10 135	23 856	24 568	11 840	11 796
R_{int}	0.0310	0.0157	0.0000	0.0196	0.0255	0.0000	0.0316
Final R_1 [a] values [$F^2 > 2\sigma(F^2)$]	0.0324	0.0205	0.0487	0.0606	0.0361	0.0615	0.0572

Compound	**3b/3b′**	**4**	**6**	**7a**	**7b**	**8b**	**9**
Final w$R(F^2)$[b] values [$F^2 > 2\sigma(F^2)$]	0.0803	0.0542	0.1287	0.1686	0.0917	0.1605	0.1491
Final R_1 [a] values (all data)	0.0528	0.0245	0.0502	0.0689	0.0489	0.0805	0.0783
Final w$R(F^2)$[b] values (all data)	0.0884	0.0562	0.1301	0.1744	0.0970	0.1719	0.1870
Goodness of fit on F^2, S[c]	1.094	1.029	1.070	1.094	1.037	1.089	1.054

a $R_1(F) = \Sigma||F_o| - |F_c||/\Sigma|F_o|$ **for observed reflections** $[F^2 > 2\sigma(F^2)]$. ***b*** $wR_2(F^2) = (\Sigma[w(F_o^2 - F_c^2)^2]/\Sigma[w(F_o^2)^2])^{1/2}$. ***c*** **GOF =** $(\Sigma[w(F_o^2 - F_c^2)^2]/(n - p))^{1/2}$**, where *n* and *p* are the number of data and parameters.**

Figure 1

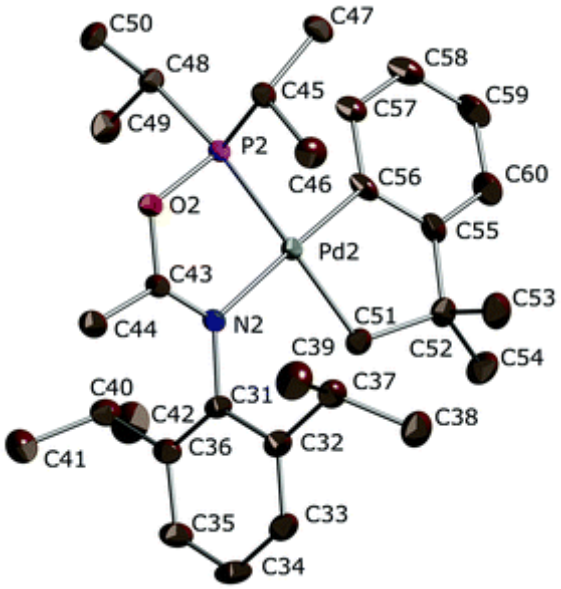
C50
C47
C48
C58
C45
C59
C57
C49
P2
C46
C56
C60
O2
C55
Pd2
C43
C53
C51
C44
N2
C52
C39
C54
C37
C40
C31
C42
C38
C36
C32
C41
C35
C33
C34

Figure 2

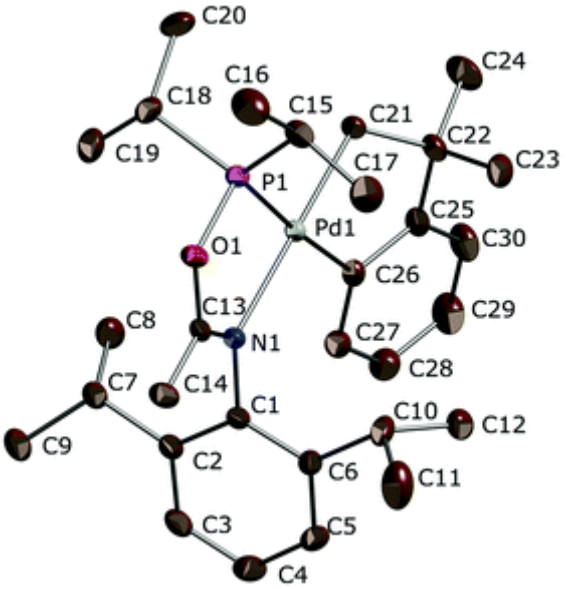
C20
C16
C24
C18
C15
C21
C22
C19
C17
C23
P1
C25
Pd1
C30
O1
C26
C13
C29
C8
N1
C27
C7
C14
C28
C1
C10
C12
C9
C2
C6
C11
C3
C5
C4

Figure 3

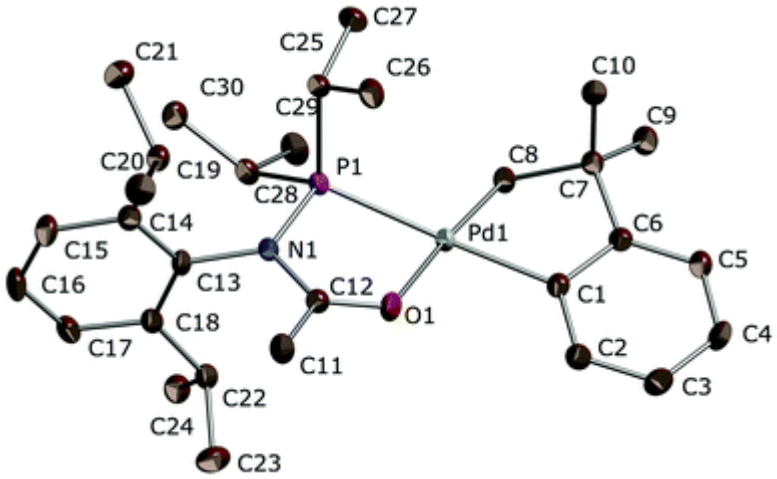
C27
C25
C21
C26
C10
C30
C29
C9
C20
C19
P1
C8
C28
C7
C14
Pd1
C6
C15
N1
C5
C16
C13
C12
C1
O1
C18
C4
C17
C2
C11
C22
C3
C24
C23

Figure 4

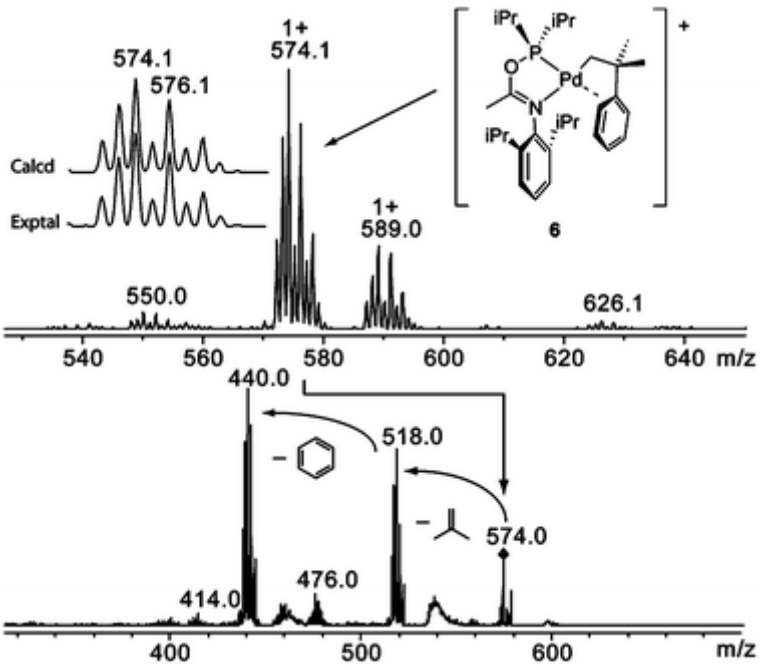
574.1
576.1
1+
574.1
Calcd
Exptal
1+
589.0
550.0
626.1
540
560
580
600
620
640 m/z
iPr
iPr
P
O
Pd
N
iPr
iPr
+
6
440.0
518.0
574.0
476.0
414.0
400
500
600
m/z

Figure 5

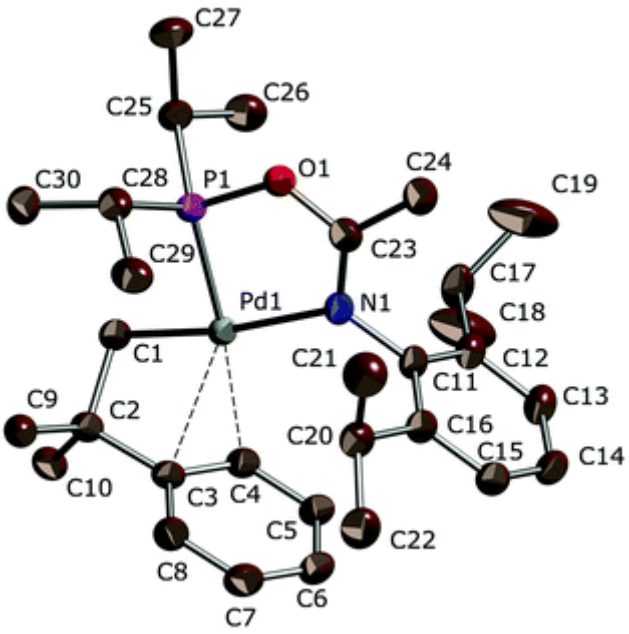
C27
C25
C26
C30
C28
P1
O1
C24
C19
C29
C23
C17
Pd1
N1
C18
C1
C21
C12
C11
C9
C2
C13
C20
C16
C15
C14
C10
C3
C4
C5
C22
C8
C6
C7

Figure 6

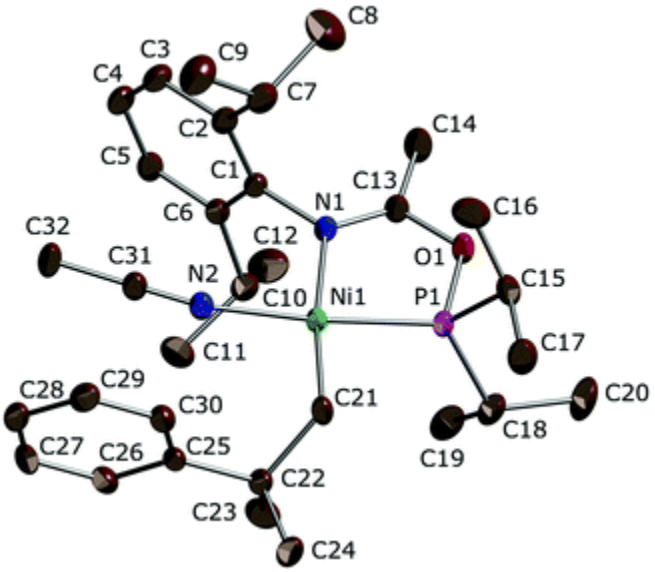
C8
C3
C9
C4
C7
C2
C14
C5
C1
C13
C6
N1
C16
C32
C12
C31
O1
N2
C10
Ni1
P1
C15
C11
C17
C28
C29
C21
C20
C30
C18
C27
C26
C25
C19
C22
C23
C24

Figure 7

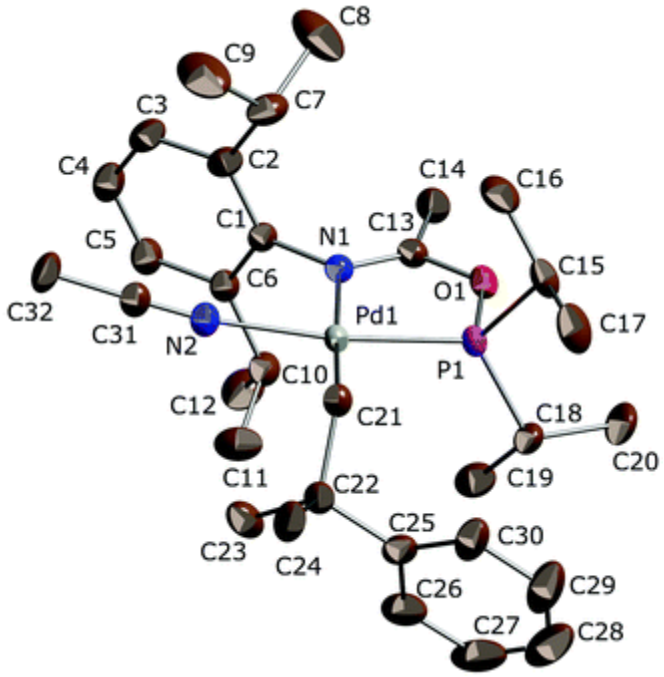
C8
C9
C7
C3
C2
C4
C14
C16
C1
C13
N1
C5
C15
C6
O1
C32
Pd1
C17
C31
N2
P1
C10
C12
C21
C18
C20
C11
C22
C19
C25
C30
C23
C24
C26
C29
C27
C28

Figure 8

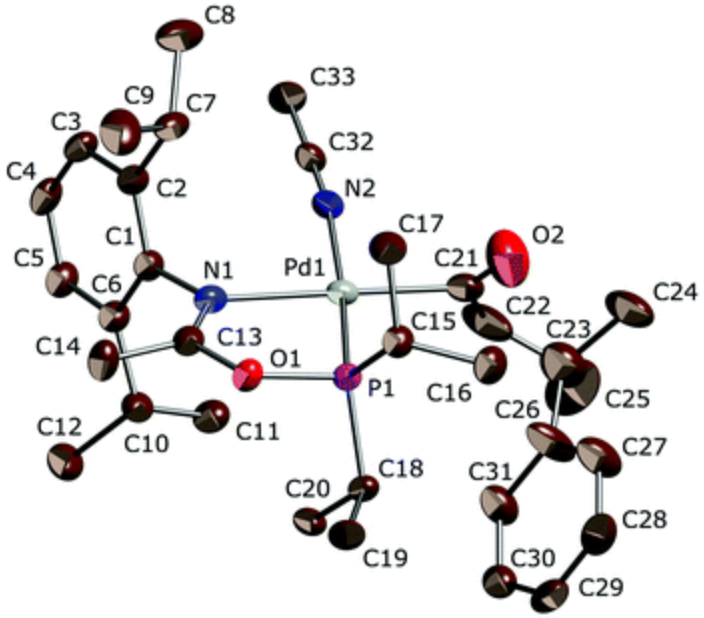
C8
C33
C9
C7
C3
C32
C4
C2
N2
C17
C1
O2
C5
N1
Pd1
C21
C6
C24
C22
C15
C23
C14
C13
O1
P1
C16
C25
C26
C12
C10
C11
C27
C18
C31
C20
C28
C19
C30
C29

Figure 9

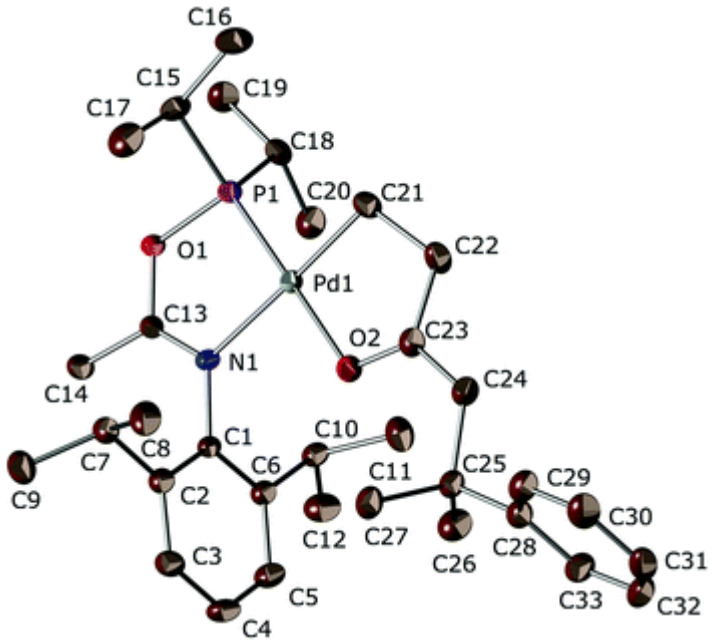
C16
C15
C19
C17
C18
P1
C20
C21
O1
C22
Pd1
C13
O2
C23
N1
C14
C24
C1
C10
C8
C7
C6
C11
C25
C29
C9
C2
C30
C12
C27
C26
C28
C3
C31
C5
C33
C32
C4

Scheme 1

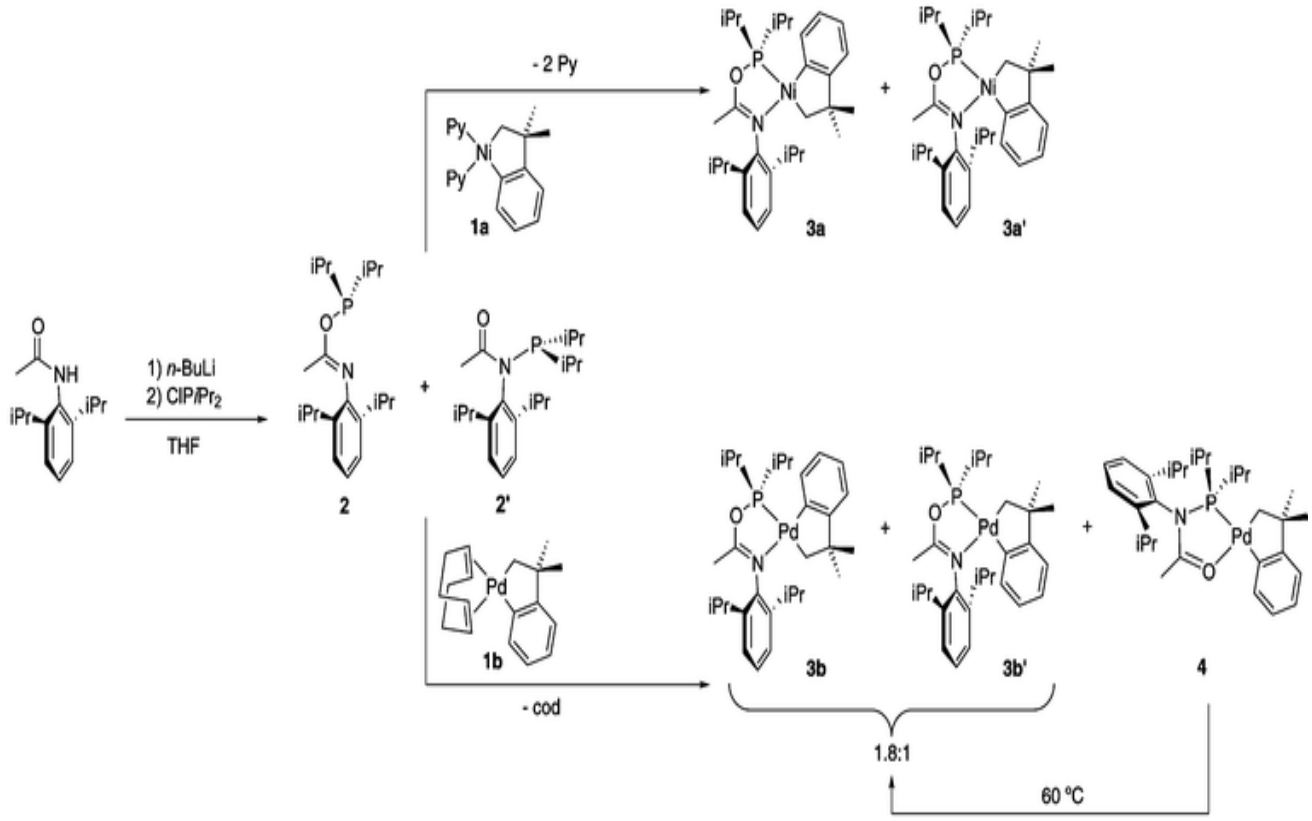

Scheme 2

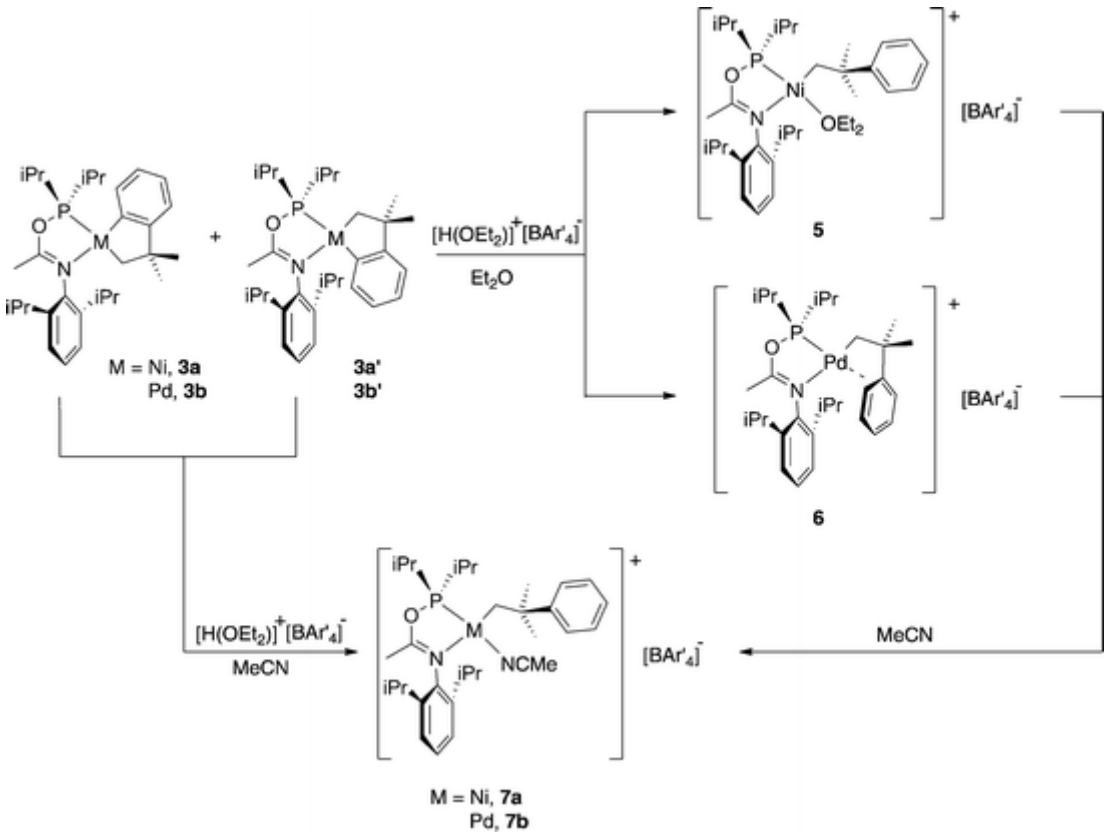

Scheme 3

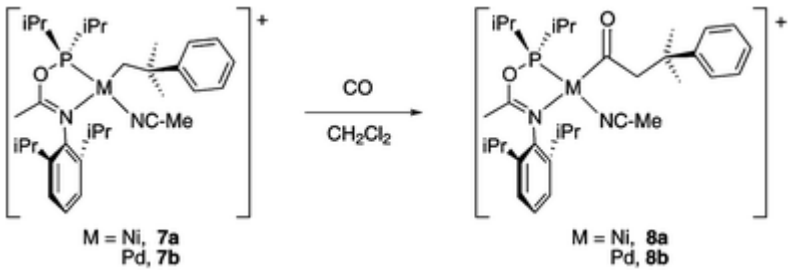

Scheme 4